NASA/TM-2006-213921
ARL-TR-3638

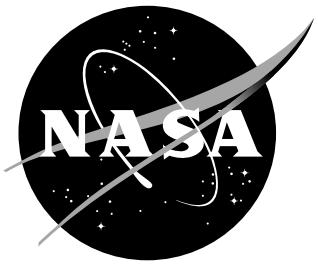

Flow Liner Slot Edge Replication Feasibility Study

John A. Newman
U.S. Army Research Laboratory
Vehicle Technology Directorate
Langley Research Center, Hampton, Virginia

Scott A. Willard
Lockheed Martin Space Operations
Langley Research Center, Hampton, Virginia

Stephen W. Smith and Robert S. Piascik
Langley Research Center, Hampton, Virginia

February 2006

The NASA STI Program Office ... in Profile

Since its founding, NASA has been dedicated to the advancement of aeronautics and space science. The NASA Scientific and Technical Information (STI) Program Office plays a key part in helping NASA maintain this important role.

The NASA STI Program Office is operated by Langley Research Center, the lead center for NASA's scientific and technical information. The NASA STI Program Office provides access to the NASA STI Database, the largest collection of aeronautical and space science STI in the world. The Program Office is also NASA's institutional mechanism for disseminating the results of its research and development activities. These results are published by NASA in the NASA STI Report Series, which includes the following report types:

- TECHNICAL PUBLICATION. Reports of completed research or a major significant phase of research that present the results of NASA programs and include extensive data or theoretical analysis. Includes compilations of significant scientific and technical data and information deemed to be of continuing reference value. NASA counterpart of peer-reviewed formal professional papers, but having less stringent limitations on manuscript length and extent of graphic presentations.

- TECHNICAL MEMORANDUM. Scientific and technical findings that are preliminary or of specialized interest, e.g., quick release reports, working papers, and bibliographies that contain minimal annotation. Does not contain extensive analysis.

- CONTRACTOR REPORT. Scientific and technical findings by NASA-sponsored contractors and grantees.

- CONFERENCE PUBLICATION. Collected papers from scientific and technical conferences, symposia, seminars, or other meetings sponsored or co-sponsored by NASA.

- SPECIAL PUBLICATION. Scientific, technical, or historical information from NASA programs, projects, and missions, often concerned with subjects having substantial public interest.

- TECHNICAL TRANSLATION. English-language translations of foreign scientific and technical material pertinent to NASA's mission.

Specialized services that complement the STI Program Office's diverse offerings include creating custom thesauri, building customized databases, organizing and publishing research results ... even providing videos.

For more information about the NASA STI Program Office, see the following:

- Access the NASA STI Program Home Page at ***http://www.sti.nasa.gov***

- E-mail your question via the Internet to help@sti.nasa.gov

- Fax your question to the NASA STI Help Desk at (301) 621-0134

- Phone the NASA STI Help Desk at (301) 621-0390

- Write to:
  NASA STI Help Desk
  NASA Center for AeroSpace Information
  7121 Standard Drive
  Hanover, MD 21076-1320

NASA/TM-2006-213921
ARL-TR-3638

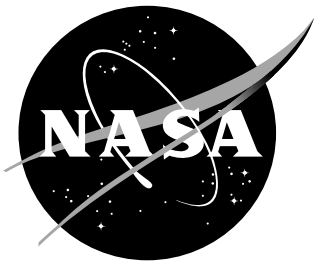

Flow Liner Slot Edge Replication Feasibility Study

John A. Newman
U.S. Army Research Laboratory
Vehicle Technology Directorate
Langley Research Center, Hampton, Virginia

Scott A. Willard
Lockheed Martin Space Operations
Langley Research Center, Hampton, Virginia

Stephen W. Smith and Robert S. Piascik
Langley Research Center, Hampton, Virginia

National Aeronautics and
Space Administration

Langley Research Center
Hampton, Virginia 23681-2199

February 2006

The use of trademarks or names of manufacturers in the report is for accurate reporting and does not constitute an official endorsement, either expressed or implied, of such products are manufacturers by the National Aeronautics and Space Administration or the U.S. Army.

Available from:

NASA Center for AeroSpace Information (CASI)
7121 Standard Drive
Hanover, MD 21076-1320
(301) 621-0390

National Technical Information Service (NTIS)
5285 Port Royal Road
Springfield, VA 22161-2171
(703) 605-6000

Abstract

Surface replication has been proposed as a method for crack detection in space shuttle main engine flowliner slots. The results of a feasibility study show that examination of surface replicas with a scanning electron microscope can result in the detection of cracks as small as 0.005 inch, and surface flaws as small as 0.001 inch, for the flowliner material.

Introduction

Cracks have been found at slots in space-shuttle orbiter main engine liquid hydrogen (LH_2) feed line gimbal-joint flowliners (refs. 1, 2). These flowliners are located in the aft end of the orbiters (See Figure 1a) inside the LH2 feedlines (See Figure 1b). Flowliners are constructed of Inconel 718 sheet material (0.05 inches thick) and are designed to provide a smooth flow of fuel over the bellows of the gimbal joint. The upstream and downstream flowliners, shown in Figure 1c, each contain 38 slots. The upstream flowliner slots are nominally 1.00 inch (25.4 mm) long and 0.25 inches (6.35 mm) wide, and the downstream slots are nominally 0.75 inches (19.1 mm) long and 0.25 inches (6.35) wide (See Figure 1d).

Cracks were initially discovered by visual examination and subsequent examination using well-established NDE (non-destructive evaluation) methods (most notably, Eddy current) were also performed. All cracks found were 0.100 inches (2.54 mm) or longer and the accepted NDE resolution is 0.075 inch (1.9 mm). All cracks that were identified were weld repaired. The possibility of multi-site damage – the existence of multiple cracks at lengths just below the detection threshold – is a concern. The specific threat that cracked flowliners presents is the release of foreign-object debris (FOD). Even a small piece of FOD could damage downstream components including fuel pumps.

To ensure flowliners are free of small cracks, an alternate inspection method is needed that can reliably detect cracks much smaller than 0.075 inch (1.9 mm). Surface replication (SR) is proposed as a method to detect cracks as small as 0.005 inch (0.127 mm). Rather than directly examine a component, SR methods rely on inspections of surface replicas to characterize the damage state. The primary advantages of SR methods are that the component is not directly analyzed and that replicas document and preserve the surface conditions corresponding to specific times during the service life. The disadvantages are that only surface damage is documented and special care must be taken to ensure that the replica is an accurate representation of the actual surface conditions. SR methods are good candidates for flowliner inspection because a direct inspection of the flowliner slots is not practical, and cracks are known to initiate on the slot surface (*i.e.*, damage is not sub-surface). Additionally, sub-critical damage can be monitored by comparison with replicas taken at different times. Occasionally, flaws in replicas may occur such that the features on the replica do not accurately mimic the actual slot surface. For this reason multiple replicas should be made for each surface, so that features found on one replica can be verified on another.

The objectives of this paper are to determine the feasibility of the proposed surface replication method to find small cracks and characterize the surface finish of the polished slots. A recently developed SR method is proposed for this application due to its ease of use. For the methods described within this report, it has been determined that this SR technique can accurately and reliably detect cracks as small as 0.005 inch.

Surface Replication Methods

Surface replication methods have been used for decades as a way to monitor the initiation and growth of small cracks (refs. 3, 4). Two surface replication methods were used in this study; acetate tape replication and a silicon-based compound commercially known as RepliSet.[1] The acetate tape method is well established and has been used extensively for decades. RepliSet is a relatively new SR method, but is much easier to use compared with acetate tape. Because this proposed method requires hundreds of replicas to be taken per vehicle, the ease-of-use advantage warrants consideration of RepliSet over the well established acetate tape method.

Acetate Tape Method

For the acetate tape method, surface replicas are made using small strips or pieces of transparent acetate tape. Replicas are made by covering the area of interest with acetate tape and applying a small amount of acetone between the component and tape. Acetone partially dissolves and softens the acetate tape and allows it to flow against the specimen. After the acetone dries, the acetate tape is removed as a replica of the surface. This procedure is illustrated in Figure 2.

RepliSet Method

RepliSet is a two-part silicon-based compound, and replicas are made by dispensing this compound into flowliner slots. The two components are kept separate in the cartridges until ready for use. When dispensed, these components flow through a static mixing nozzle where they are mixed before filling the flowliner slots, as shown in Figure 3. After a 10-minute cure, the RepliSet replica is ready to remove. The Repliset compound is dispensed into the slots and, because this compound is viscous, is held in place with tape until it is cured. In Figure 3, Repliset is being dispensed into the slot of a test specimen (left side) filling it completely. The slot on the right side has already been filled with Repliset which is held in place with tape. For this study the RepliSet compound T3 was used which had a working time of approximately 3 minutes and a curing time of 10 minutes.

Experimental Procedure

The simulation of cracks at flowliner slots was accomplished by fatigue testing specimens containing slots with the same dimensions as an upstream flowliner under fatigue loading. Two types of specimens used, shown schematically in Figure 4, were provided by NASA Marshall Space Flight Center. Both specimen types were constructed of the same 0.05-inch-thick Inconel 718 sheet product used for the flight hardware. The slots in all specimens were punched and polished using procedures similar to those of flight hardware. Double-edge notch specimens ($k_t = 3.55$) were fatigue tested at $R = 0.1$ and a maximum load of $P_{max} = 4.5$ kips, which corresponds to a notch stress of 160 ksi.[2] To achieve the same notch stresses (160 ksi), center-slot specimens ($k_t = 3.52$) were fatigue loaded at $P_{max} = 3.35$ kips ($R = 0.1$). Fatigue tests were performed in room temperature laboratory air at loading frequencies ranging from 5 Hz to 10 Hz. Periodically, testing was stopped while slot surface replicas were made using both replication methods (RepliSet and acetate tape). Replicas were produced with the specimen under either zero applied load or at the maximum applied load. It is presumed that any crack would be more readily detected using a replica taken at the maximum load because any crack present would be fully open. Comparing the results (crack lengths) determined from zero-load and maximum load replicas will help determine if crack length determinations are dependent upon the loading condition.

[1] RepliSet is a trademark of Struers.

[2] The stress concentration factors presented here are based on the gross-section stress – the average gage-section stress that would exist if the notches were not present.

Specimens were fatigue loaded, and periodically replicated, until small cracks were detected. Multiple specimens were cracked to develop a specimen set with a good distribution of cracks ranging in size from 0.005 inch to 0.025 inch (0.127 mm to 0.635 mm). For each specimen, crack length determinations were made using (1) acetate tape replicas, (2) RepliSet replicas, and (3) destructive specimen examination using a scanning electron microscope (SEM). Comparing results over a wide range in crack lengths and loading conditions will help determine if there are conditions where RepliSet crack length determinations are inadequate.

All of the flowliner slots have been polished following the discovery of cracks in 2002 (ref. 2). Due to the possibility that slots containing small undetected cracks were polished, it is important to determine how this affects crack detection. Also, if polishing is used to eliminate small cracks, replicas will be used to ensure that the entire crack has been removed. Cracked specimens will be polished to a depth of approximately 0.002 inch (0.05 mm) using the same procedures used on the flight hardware, and will be analyzed as previously discussed.

Experimental Results

Crack detection

All crack length determinations from the test specimens are summarized in Table 1. Here, the length of each crack detected, using both replica methods and direct SEM examination of each specimen, are listed (some specimens contain multiple cracks). Should the RepliSet method lack the resolution to replicate crack features, the crack length values would be expected to be consistently less than for the other two methods. No such trend is seen in these data although there does appear to be some variability. A qualitative comparison of the RepliSet method can be made by comparing SEM micrographs of the same features. Comparisons are made for several specimens in the following sections.

Specimen P1

Specimen P1 was the first specimen tested and was originally fatigue loaded at a notch stress of 140 ksi (R = 0.1). After 147,000 cycles no cracks were detected and loads were increased to a notch stress of 160 ksi. All other specimens were strictly loaded at a notch stress of 160 ksi and R = 0.1. Three cracks were detected on replicas made at a cumulative cycle count of 270,000 (123,000 cycles at 160 ksi notch stress). The largest crack was a corner crack with an approximate length of 0.014 inch (350 μm). Two smaller surface cracks of lengths 0.004 inch (110 μm) and 0.001 inch (27 μm) were also detected.[3] The large crack can be seen in an SEM image of an acetate tape replica. See Figure 5a. The two smaller cracks can be seen at higher magnification (Figure 5b).

The slot surface was replicated using both replica methods. Additionally, cracks were detected by directly examining the slot surfaces in an SEM. To characterize the crack detection capability of Repliset, SEM images of Repliset will be compared with similar images of acetate replicas (a well-established and trusted method) and a direct examination of the slot surface. Cracks are more likely to be detected on replicas taken under an applied tensile load because the cracks are open. In this comparative study, acetate tape replicas were taken at maximum load (160 ksi notch stress). Repliset replicas were taken on unloaded specimens because this stress state is believed to better represent the stress state of the flowliners during inspections.

[3] The length of corner cracks (typically denoted as '*c*' in the technical literature) is the distance from the corner to the crack tip. Surface crack lengths (denoted as '2*c*') is the distance between the two crack tips.

Table 1. Crack length measurements from replicas and specimen examinations. Values of length are given in μm. Specimens beginning with P and C correspond to double-edge notch and center notch specimens, respectively.

Specimen ID	Crack #	Crack Length (μm)			
		RepliSet zero load	**Acetate Tape** zero load	**Acetate Tape** max load	**Destructive Exam** zero load
P1	1	343	230	280	236-350
	2	104	90	81	110
	3	26	22	20	27
P2	1	137	1353	132	143
C3	1	199	185	183	194
C5	1	252	224		237
	2	327	186		305
C6	1	170	159	163	171
	2	218	200	206	218
	3	170	164	162	170
	4	201	204	193	201
	5	211	196	206	211
	6	45	42	43	45
	7	156	157	149	156
C8	1	129	118	131	140
	2	249	208	226	250

SEM micrographs of crack #1 are shown for an acetate tape replica taken at max load (Figure 6a), a Repliset replica taken at zero load (Figure 6b), and of the actual specimen (Figure 6c) also taken at zero load.[4] A qualitative comparison shows that the same subtle crack features appear in all three images. From the acetate tape replica the crack length was determined to be 0.0110 inches long (280 μm). The result from the Repliset was 0.0135 inches (343 μm). The crack length from the specimen, somewhat difficult to determine because the crack tip was difficult to locate, was in the range of 0.0093-0.0138 inches (236-350 μm). Here the Repliset method, which was handicapped because replicas were taken at zero load, indicated a longer crack was present than the acetate tape method. This 22% difference suggests that features are shown on Repliset replicas that are missed on the acetate tape replicas.

Images for cracks #2 and #3 are shown in Figures 7 and 8, respectively. For crack #2, the crack lengths determined from the acetate tape (Figure 7a), Repliset (Figure 7b), and the specimen (Figure 7c) are 0.0032 inch (81 μm), 0.0041 inch (104 μm) and 0.0043 inch (110 μm), respectively. Here, the acetate tape crack determination is approximately 22% less than the Repliset determination, and both replica measurements are less than the specimen indication. For crack #3, the crack length measurements for

[4] Images taken from replicas are mirror images of the actual specimen. For better comparison, images have been flipped such that features on the right-hand-side of the replica images correspond to features on the right-hand-side of the specimen images.

acetate tape (Figure 8a), Repliset (Figure 8b), and the specimen (Figure 8c) are 0.0010 inch (26 μm), 0.0008 inch (20 μm), and 0.0011 inch (28 μm), respectively. Again, the Repliset crack length measurement is greater than the acetate tape value, but slightly less than from a destructive specimen examination.

Specimen P2

Specimen P2 was fatigue loaded at a notch stress of 160 ksi (R = 0.1). After 115,000 cycles a 0.005-inch-long surface crack was found. As shown in Figure 9a, crack initiation occurred near the mid-thickness of the slot. This crack is shown at higher magnification in Figure 9b. SEM images of this crack are shown for an acetate tape replica (Figure 10a), Repliset (Figure 10b), and the specimen (Figure 10c). A comparison of these images reveals that the qualitative features (e.g., shape of the crack) in each image are similar to the other images of the same crack. Comparison of the crack length measurements reveals that the Repliset measurement of 0.0054 inch (137 μm) is bounded by the acetate tape measurement of 0.0052 inch (132 μm) and the destructive examination value of 0.0056 inch (143 μm).

Specimen C3

After 165,000 cycles at a notch stress of 160 ksi, a 0.008-inch-long surface crack was found in specimen C3. This crack is shown at low magnification in Figure 11a and at higher magnification in Figure 11b. SEM images of this crack obtained from acetate tape (max load), Repliset (unloaded), and the specimen (unloaded) are shown in Figures 12a, 12b, and 12c, respectively. In all three images the cracks appear to be remarkably similar. The crack length determination from acetate tape is 0.0072 inch (183 μm), and the determination from Repliset is 0.0078 inch (199 μm). Again, the Repliset crack length determination is slightly longer than the acetate tape value, despite the disadvantage of being taken in the unloaded state. Curiously, the Repliset crack length measurement is slightly longer than the value from the destructive exam, which is 0.0076 inch (194 μm).

Specimen C6

Specimen C6 was fatigue loaded at a notch stress of 160 ksi (R = 0.1). At 50,000 cycles at least seven fatigue cracks were found as indicated in Figure 13. Presumably these cracks initiated at pit-like damage sites that were not completely removed during the polishing process. The effect of surface finish on fatigue life will be discussed later in this paper. Each crack is shown at higher magnification using acetate tape replicas, Repliset replicas, and the through direct examination of the specimen (See Figures 14-20).

Images of crack #1, a 0.006-inch-long surface crack are shown in Figure 14. In all three images, the pit-like damage is readily seen with the fatigue crack growing out on both sides. The crack length determinations from acetate tape, Repliset, and a specimen examination are 0.0064 inch (163 μm), 0.0067 inch (170 μm), and 0.0067 inch (171 μm), respectively.

Images of crack #2, a 0.008-inch-long surface crack are shown in Figure 15. In all three images, the pit-like damage is readily seen in the center of each image, with the fatigue crack growing out on both sides. The crack length determinations from acetate tape, Repliset, and a specimen examination are 0.0081 inch (206 μm), 0.0086 inch (218 μm), and 0.0086 inch (218 μm), respectively.

Images of crack #3, a 0.006-inch-long surface crack are shown in Figure 16. In all three images, a small amount of pit-like damage is seen on the far right of the image with the fatigue crack propagating towards the left. The crack length determinations from acetate tape, Repliset, and a specimen examination are 0.0064 inch (162 μm), 0.0067 inch (170 μm), and 0.0067 inch (171 μm), respectively.

Images of crack #4, a 0.008-inch-long surface crack are shown in Figure 17. In all three images, two regions of pit-like damage are seen, one near the center of the images and another on the far right side of the images. It is not known if crack #4 is the result of a single crack that initiated at one damage site and propagated to the other, or if it is the results of two smaller cracks that grew together to form a larger crack. The crack length determinations from acetate tape, Repliset, and a specimen examination are 0.0076 inch (193 μm), 0.0079 inch (201 μm), and 0.0079 inch (201 μm), respectively.

Images of crack #5, a 0.008-inch-long surface crack are shown in Figure 18. In all three images, a small pit-like damage site is readily seen near the center of each image, with the fatigue crack growing out on both sides. The crack length determinations from acetate tape, Repliset, and the specimen are 0.0081 inch (206 μm), 0.0083 inch (211 μm), and 0.0083 inch (211 μm), respectively.

Images of crack #6, a 0.002-inch-long surface crack are shown in Figure 19. In all three images, a cluster of pit-like damage sites are readily seen in the center of each image. The fatigue crack can be seen primarily growing on the left side of the damage zone. The crack length determinations from acetate tape, Repliset, and a specimen examination are 0.0017 inch (43 μm), 0.0018 inch (45 μm), and 0.0018 inch (45 μm), respectively.

Images of crack #7, a 0.006-inch-long surface crack are shown in Figure 20. In all three images, pit-like damage is readily seen on the far right side of each image, with the fatigue crack propagating toward the left. The crack length determinations from acetate tape, Repliset, and a specimen examination are 0.0059 inch (149 μm), 0.0061 inch (156 μm), and 0.0061 inch (156 μm), respectively. For all seven cracks in specimen C6, the crack length determinations obtained from the acetate tape replicas were less than the Repliset values, and the Repliset values were nearly the same as the crack lengths determined by destructive examination.

Specimen C8

Specimen C8 was fatigue loaded at a notch stress of 160 ksi (R = 0.1). At 50,000 cycles two surface cracks were found as indicated in Figure 21a. Crack #1, a 0.008-inch-long surface crack, is shown at higher magnification in Figure 21b, and crack #2, a 0.005-inch-long surface crack, is shown at higher magnification in Figure 21c. Each of these cracks is shown at higher magnification using acetate tape replicas, Repliset replicas, and the actual specimen, as was done for the previous specimens. For each of the images of crack #1 (acetate replica, Repliset replica, and direct imaging of the specimen) shown in Figure 22, a small amount of pit-like damage can be seen near the center of the image with the crack propagating on either side. The crack length determinations from acetate tape, Repliset, and a specimen examination are 0.0089 inch (226 μm), 0.0098 inch (249 μm), and 0.0098 inch (250 μm), respectively. A small amount of pit-like damage has also been revealed for the three different images produced for crack #2 (See Figure 23). The crack length determinations from acetate tape, Repliset, and a specimen examination are 0.0052 inch (131 μm), 0.0051 inch (129 μm), and 0.0055 inch (140 μm), respectively. Unlike any of the other previous examples, here the acetate tape crack length is slightly larger (approximately 2% difference) than the Repliset value.

Reproducibility

A limited amount of slot surface replication was also performed using a dental molding material that is approved for use on flight hardware. However, replication of slot surfaces using dental mold was discontinued after it was discovered that small quantities of this material was left in the crack mouth upon replica removal. After repeatedly using this replication media, cracks became clogged with foreign material and were much more difficult to locate. Although there was no evidence that Repliset may create a similar problem, a study was performed to determine if repeated application of this media would

result in foreign material entrapment in the crack mouth. The slot surface of specimen C6 was replicated using Repliset five times. In Figure 24, SEM images are shown for crack #3 on specimen C6; (a) an image of an acetate replica, (b) image of the first Repliset replica, and (c) image of the fifth Repliset replica. No significant differences are seen between these images and no accumulation of foreign material is observed in the crack mouth in Figure 24c. Similar findings are reported for crack #4 on specimen C6, as show in Figure 25, and for the other five cracks of specimen C6, although further results are not presented in this report for brevity.

Post-polish crack detection

Experimental results show that polishing of cracked surfaces increases the difficulty of crack detection, especially for soft ductile materials such as aluminum. The possibility of something similar occurring in Inconel 718 is worthy of consideration, especially considering that polishing is a proposed method for removal of small cracks. If the Repliset method is unable to detect existing cracks after slot surfaces are polished, it may be impossible to determine if the crack has been completely removed or is simply undetectable. To determine how polishing affects crack detection, several specimens containing a wide range of crack shapes and sizes were replicated before and after polishing. In all cases, specimens were polished using the flight-hardware-approved method and replicas were taken in the unloaded condition.

Specimen C1

Specimen C1 was fatigue loaded at a notch stress of 160 ksi (R = 0.1) for 75,000 cycles. By this time a fatigue crack had initiated and propagated to a through-thickness crack that was approximately 0.145 inches deep (about 3 times the sheet thickness). The through-thickness crack can be seen in the SEM image of an acetate tape replica shown in Figure 26a. This crack appears to have a jog or discontinuous change between the regions labeled (b) and (c), which is consistent with the initiation of multiple cracks or damage sites and the subsequent coalescing of cracks as they grow together. Higher magnification images of regions (b) and (c) are shown in Figures 26b and 26c, respectively. This crack is clearly a through-thickness crack because it is seen propagating around both corners.

The slot was then polished, removing approximately 0.002 inches (0.05 mm) of material. Replicas were taken of the previously cracked area, and the crack was still detected on a Repliset replica, as shown in Figure 27a. It should be noted that the crack is much less pronounced following the polishing procedure. Higher magnification images of the regions labeled (b), (c), and (d) are shown in Figures 27b, 27c, and 27d, respectively. The crack is found to be continuous across the entire surface when examining the higher magnification images (See Figures 27b through d). Therefore, this crack can be detected and is recognized as a through-thickness crack using Repliset replicas after polishing.

Specimen C2

Specimen C2 was fatigue loaded at a notch stress of 160 ksi (R = 0.1) for 50,000 cycles. A fatigue crack initiated and propagated to a through-thickness crack that was 0.015 inches deep on one side and 0.023 inches deep on the other (less than 50% of the sheet thickness). The through-thickness crack can be seen in the SEM image of an acetate tape replica shown in Figure 28a. Higher magnification images of the regions labeled (b), (c), and (d) are shown in Figures 28b-d, respectively. In these images a continuous crack can be seen rounding both corners and is therefore identified as a through-thickness crack.

Following the identification of the through-thickness crack, the slot was polished, removing approximately 0.002 inches (0.05 mm) of material. The crack can still be detected on a Repliset replica, as shown in Figure 29a, although the crack is much less pronounced after polishing. Higher

magnification images of the regions labeled (b), (c), and (d) are shown in Figures 29b-d, respectively. Here, the crack can be observed to be continuous across the entire slot surface. Therefore, after polishing this crack can be detected and is recognized as a through-thickness crack using Repliset replicas.

Specimen C9

Specimen C9 was fatigue loaded at a notch stress of 160 ksi (R = 0.1) for 64,000 cycles. A fatigue crack initiated and propagated to become a corner crack measuring 0.039 inches (833 μm) in length on the slot surface and 0.015 inches (380 μm) in length on the side of the specimen. An SEM micrograph (acetate tape replica) of the slot surface is shown as Figure 30a. The crack is seen to have propagated from one corner (region (b)) through nearly 80% of the sheet thickness (to region (c)). Higher magnification images of regions (b) and (c) are shown in Figure 30b and 30c, respectively. Figure 30b reveals that the crack has propagated around the edge on the left. The crack tip is shown in Figure 30c, indicating that the crack has yet to grow to the corner on the right side. Therefore this crack is identified as a corner crack (i.e., propagated around one corner) rather than a through-thickness crack (i.e., propagated around both corners).

The slot surface was polished, removing approximately 0.002 inches (0.05 mm) of material. The crack can still be detected on a Repliset replica, as shown in Figure 31a, although the crack is much less pronounced than before. Higher magnification images of the regions labeled (b), (c), and (d) are shown in Figures 31b-d, respectively. The crack can be readily identified from the left-side corner to at least 50% through the sheet thickness (0.025 inches). It is difficult to identify the crack tip and quantify the crack size. However, this crack remains detectable after polishing and is identified as a corner crack. A small crack-like feature is shown in Figure 31d, although no connection is found with the previously mentioned corner crack.

Specimen C12

Specimen C12 was fatigue loaded at a notch stress of 160 ksi (R = 0.1) for 50,000 cycles. A 0.022-inch-long (560 μm) surface crack was found on the slot surface of this specimen. SEM micrographs of this crack are shown in Figure 32. As indicated in Figure 32a, the crack is to the left of center in the region labeled (b). A high magnification image of this crack is shown in Figure 32b. After polishing away approximately 0.002 inches (0.05 mm) of material from the slot, this crack was not detected. Assuming a semi-circular aspect ratio, the expected depth of this crack was originally 0.011 inch, and after polishing is expected to be approximately 0.009 inches deep.

Specimen C13

Specimen C13 was fatigue loaded at a notch stress of 160 ksi (R = 0.1) for 50,000 cycles. A 0.019-inch-long (480 μm) surface crack was found on the slot surface of this specimen. SEM micrographs of this crack are shown in Figure 33. As indicated in Figure 33a, the crack is to the left of center in the region labeled (b). A high magnification image of this crack is shown in Figure 33b. After polishing away approximately 0.002 inches (0.05 mm) of material from the slot, this crack was not detected. Assuming a semi-circular aspect ratio, the expected depth of this crack was originally 0.0095 inch, and after polishing is expected to be approximately 0.0075 inches deep.

Crack Loading

Although the small surface cracks of Specimens C12 and C13 were not detected after polishing, these cracks could be detected after the cracks were reopened by the application of tensile loading. For example, SEM images of Specimen C12 (Repliset replica) are shown in Figure 34a for an applied tensile load corresponding to a notch stress of 50 ksi. The crack can be seen in the higher magnification image

of the crack region (labeled (b)) shown as Figure 34b. SEM images of specimen C13 (Repliset replica) are shown in Figure 35a for the specimen loaded to a notch stress of 50 ksi. This crack can also be seen at higher magnification, as shown in Figure 35b.

Surface finish characterization

During the fatigue-cracking portion of this study a correlation between slot surface finish and initiation cycles was observed. Specifically, the crack initiation life was shorter for slots with a higher concentration of defects. The majority of flaws encountered on the slot surfaces are artifacts of the slot punching process. A micrograph of an unpolished as-punched slot (acetate tape replica) is shown in Figure 36. Here, the punch penetrated the Inconel 718 sheet from the left. This punching process creates visible damage on the slot surface that appears to have a pit-like morphology and is especially severe on the exit-side of the sheet (right side of Figure 36). This high degree of surface roughness is undesirable from a crack initiation perspective and the laboratory testing performed in this study has indicated that a higher concentration of surface flaws will result in shorter crack initiation life. For this reason, all flowliner slots have been polished since the discovery of cracks, whether the slot was found to have any cracks or not. However, laboratory experience suggests surface finish quality will vary significantly in the polished specimens despite each slot being polished using the flight-hardware-approved method.

Consider the SEM images (acetate replicas) of four polished slot surfaces shown in Figure 37. All slot surfaces were polished in accordance with the flight-hardware-approved method and the images shown in Figure 37 correspond to the specimen condition prior to fatigue loading. A high-quality surface finish is show in Figure 37a meaning that no visible flaws or pits are seen on the slot surface. A limited amount of damage is indicated in Figure 37b. Here, a few individual pits exist but are spaced sufficiently far apart such that interactions between these stress raisers does not occur. A slightly more severe damage state is shown in Figure 37c; here, a few clusters containing multiple pits exist. Within each cluster, pits are spaced sufficiently close that locally high stress states about the pits are likely to interact and may be more damaging than the presence of a single larger pit. A worse surface finish is shown in Figure 37d; here, an entire region of the slot surface (right side of the image) is densely populated with pits. This condition is described as widespread pit damage, and experimental results suggest a direct correlation between an increase in pit-like damage and a reduction in crack initiation life.

To highlight the effect of surface finish on crack initiation life consider the SEM micrographs shown in Figure 38. Figure 38a is an SEM micrograph (acetate replica) of specimen P2. Initially this specimen had a high quality surface finish with no visible flaws detected at low magnification (50X-100X), and was most nearly like the condition of Figure 37a. After 115,000 load cycles at a notch stress of 160 ksi, a single 0.005-inch-long surface crack was found, as indicated by the arrow. An SEM micrograph (acetate replica) of Specimen C8 is shown in Figure 38b. The initial surface finish of specimen C8 was somewhere between those shown in Figures 37b and 37c, characterized as mostly single non-interacting pits with an occasional multi-pit cluster. For the same notch stress state (160 ksi), only 50,000 load cycles were required to grow two surface cracks, 0.008 inches long and 0.005 inches long. An SEM micrograph (acetate replica) of Specimen C6 is shown in Figure 38c. The initial surface finish of specimen C6 was somewhere between those shown in Figures 37c and 37d, characterized as multi-pit clusters, but not quite widespread damage. For the same notch stresses, at least seven surface cracks (ranging in length from 0.008 inches to 0.002 inches) were found after 50,000 load cycles. For the same notch stresses applied to a specimen with a slot surface in the as-punched condition (recall Figure 36), on two occasions though cracks were reported by 25,000 load cycles. For a notch stress of 160 ksi, the crack initiation life for well-polished slot surface is longer than the corresponding life of an as-punched slot surface by a factor of 4 or greater.

Small crack growth data

Replicas have been used to monitor the growth of small cracks and obtain crack growth data for small cracks (refs. 3, 4). Although this was not the major objective of this work, enough crack growth history (crack length versus cycle count data) exists to determine crack growth rates as a function of crack tip driving force (ΔK). For small crack growth increments it is reasonable to assume a linear crack growth rate between two crack length observations such that the crack growth rate can be estimated as,

$$\frac{\mathrm{d}\,a}{\mathrm{dN}} = \frac{\Delta a}{\Delta\,\mathrm{N}} = \frac{\left(a_{\mathrm{i+1}} - a_{\mathrm{i}}\right)}{\left(\mathrm{N}_{\mathrm{i+1}} - \mathrm{N}_{\mathrm{i}}\right)} \tag{1}$$

Here, crack growth rate can be determined using data of crack length a_i and load cycle N_i for various observations. The cyclic crack-tip driving force, ΔK, is calculated as,

$$\Delta\mathrm{K} = \Delta\mathrm{S}\cdot\,\mathrm{F}\cdot\sqrt{\pi\,a} \tag{2}$$

where ΔS is the cyclic notch stress (σ_{net} x k_t), and the geometry correction factor, F, is assumed to be a constant equal to 0.73 (ref. 5). For the load conditions used in this study, ΔS = 144 ksi (993 MPa). The average of starting and ending crack length values ((a_{i+1} + a_i)/2) was used to compute ΔK. The raw data (crack length versus cycle count) are listed in Table 2 and the corresponding d*a*/dN-versus-ΔK data, calculated using Equations 1 and 2, are plotted in Figure 39. Long crack data are also shown for R = 0.1 and a constant-K_{max} = 33 MPa√m loading conditions (ref. 1). The scatter or variability associated with the small crack data is typical of similar data reported in the literature (ref. 6), but generally it appears that the small crack data are bounded by the two long crack curves. This means that for the same R = 0.1 load conditions, small cracks generally exhibit higher fatigue crack growth rates than long cracks, an observation that is consistent with the bulk of small crack publications (ref. 6). However, the small crack growth rates are generally less than the constant-K_{max} long crack data. Constant-K_{max} testing is useful because near threshold crack growth data are obtained at a high load ratio such that crack closure effects are eliminated. No crack closure was detected for the constant-K_{max} data shown in Figure 39. A possible explanation for differences between small crack and long crack behavior relates to crack face contact,

Table 2. Crack-length-versus-cycle-count data determined from replica analysis.

Cycle count	2a (μm) for #1	2a (μm) for #2
215,000	22	
220,000	31	
225,000	38	
230,000	52	
235,000	60	
240,000	70	14
245,000	99	32
250,000	104	46
255,000	168	55
260,000	194	60
265,000	225	77
270,000	282 (corner crack)	104

called crack closure (ref. 7). Crack closure reduces the effective crack-tip driving force. Small cracks do not have a fully developed crack wake and tend to have lower crack closure levels than long cracks. As a result, short cracks tend to have higher effective crack-tip driving forces (compared with long cracks) even though the applied crack-tip driving force is equivalent.

Destructive examination of small cracks

Most engineering analysis of small cracks assume that surface cracks have a semi-circular shape and corner cracks have a quarter-circular shape. It is likely that similar assumptions will be made in fatigue life analyses of the flowliners. To determine if this assumption is reasonable, several specimens containing small cracks were broken open to allow an inspection of the crack surfaces. A crack surface image of specimen P1 is shown in Figure 40. Recall that this specimen contained three cracks; a corner crack approximately 343 μm long and two surface cracks, 104 μm long and 26 μm long, respectively. This specimen was broken open to expose the surfaces of the corner crack and one of the surface cracks (104 μm long), as seen in Figure 40. A change in morphology separates the surface produced by fatigue from the overload failure and is shown in the figure as a dotted line. The corner crack, seen in the lower right corner of the figure, appears to have the shape expected of a surface crack (semi-circular). Here, the crack length is 343 μm and the crack depth is 176 μm. This is likely because this crack initiated as a surface crack and then propagated to the corner and the fatigue test was stopped before the crack shape could transition from a semi-circular surface crack to a quarter-circular corner crack. The smaller surface crack, seen in the lower left corner of the figure, is nearly semi-circular with a surface length of 104 μm and a depth of 55μm.

The crack surface of specimen C9 is shown in Figure 41. Recall that specimen C9 contained a large corner crack (833 μm long) and was re-polished after the fatigue test was stopped. Here, the crack shape is nearly semi-circular (crack length of 833 μm and a crack depth of approximately 342 μm) which is typical of a surface crack. This suggests that this crack initiated as a surface crack and had not reached a steady state corner crack configuration (quarter-circular) before the fatigue test was stopped. Considering that the crack surface length was approximately 80% of the sheet thickness, it seems unlikely that a steady state corner crack configuration would have been reached before the crack became a through crack.

Based on crack surface observations, it seems reasonable to assume that the depth of a surface crack is approximately one-half of its surface length. The assumption that the depth of a corner crack is equal to its surface length seems to be inaccurate, but conservative.

Discussion

The main points of discussion are as follows:

Point #1 – The Repliset method can find small cracks (<0.005 inch) and surface defects (<0.001 inch).

In this study, 14 cracks (in 5 specimens) were measured using three crack measurement techniques. Crack length determinations were made using (1) acetate tape replicas taken at maximum load (160 ksi notch stress) and on unloaded specimens, (2) Repliset replicas taken on unloaded specimens, and (3) direct specimen examinations of unloaded specimens. The acetate tape replica method is known to give acceptable results and crack detection should be enhanced because replicas were taken under tensile loading conditions. Despite the perceived advantage of tensile loading, crack length values determined

from acetate tape replicas were consistently shorter than the Repliset values. This suggests that the loading state is not critical for crack detection. There was only a single exception to this observation for each of the 14 cracks analyzed. This suggests that some near-crack-tip features that are transferred to the Repliset replicas are not reproduced on the corresponding acetate tape replicas. Of the 14 cracks observed on these specimens, one was 0.002 inches long and two were 0.005 inches long. Although no probability of detection study has been conducted for the Repliset method, clearly this method can reliably be used to locate cracks well below the accepted NDE threshold (0.075 inches). Pit-like flaws, a typical surface defect on flowliner slots, as small as 0.001 inch have been observed even at relatively low magnification (50X-100X, See Figure 37).

Point #2 – The Repliset method can distinguish between types of damage modes and the location of damage.

A significant advantage of the Repliset method is that information regarding the damage mode (*e.g*., crack, pit-like surface flaw, scratch, *etc*.) and the location of the damage are readily available. It has been shown in this document that Repliset can distinguish between crack damage (Figures 5-35) and pit-like surface flaws (Figures 36-38). Although not discussed in this document, other forms of slot surface damage can be determined including scratches, tool marks, dents, etc. Additionally, by preserving the orientation information with each replica, information is available about the damage location and configuration. In Figures 5-38 information was available about the location and severity of damage. For example, in the case of crack damage, information about the location on the slot surface and the crack configuration (*e.g*., through-thickness crack, corner crack, or surface crack) was available.

Point #3 – Cracks are more difficult to detect after polishing, but this method has been shown able to resolve cracks smaller than the accepted NDE limits.

The results shown in Figures 26-35 indicate that cracks are more difficult to detect immediately following polishing of the slot surfaces. Through-thickness cracks (Figures 26-29) and corner cracks (Figures 30-31) can still be detected after polishing, but this is not true for small surface cracks, at least in the unloaded state (Figures 32 and 33). Small surface cracks become detectable as tensile loading is applied to the specimen, as shown in Figures 34 and 35, and these cracks remain detectable even after the specimens are unloaded again.

Point #4 – The quality of slot surface finish affects the crack initiation life.

The flight-hardware approved polishing procedure has been shown to result in slot surfaces that vary in the quality of surface finish (See Figure 37). This variation in surface finish is significant because a direct correlation has been made with the crack initiation life, as shown in Figure 38. Here, all specimens were fatigue loaded at the same notch stresses, yet the cycle count to crack initiation differs significantly. For a high-quality surface finish, 115,000 cycles were required to generate a 0.005-inch-long surface crack (recall Figure 38a). For slot surfaces the contained some pit-like damage, multiple cracks of similar size (0.005 inches) occurred by 50,000 cycles (recall Figures 38b and 38c). This indicates that the presence of even a small amount of pit-like damage will reduce the crack initiation life by more than a factor of 2. The results for unpolished (as-punched) slot surfaces is yet worse; through cracks (considerably larger than 0.005-inch-long surface cracks) were found by 25,000 cycles. These observations indicates that, for the loads considered, polishing of as-punched slot surfaces will increase the crack initiation life by at least a factor of 2, even if some pit-like damage remains. Removal of all pit-like damage will provide another factor-of-2 increase in the crack initiation life.

Point #5 – Typical assumptions regarding the shape of small cracks are reasonable or conservative.

Specimens containing fatigue cracks were destructively examined to determine the aspect ratio of small cracks in this material. The depth of surface cracks was approximately one-half of the surface length, but the depth of corner cracks was significantly shorter than the surface length, likely due to the fact that the cracks observed were transforming from surface cracks to corner cracks. The assumption that the depth of corner cracks is equal to the surface length would be conservative.

Summary

A feasibility study has been conducted to determine if Repliset, a surface replication method, is a practical way to characterize damage found at space-shuttle main-engine LH_2 flowliner slots. Experimental testing was performed on coupon specimens that simulate the stress state at flowliner slots, and results have shown that the Repliset method is at least as reliable as another well-established and trusted replication method (acetate tape). On five specimens discussed in this document, fourteen cracks ranging from 0.002 inches long to 0.008 inches long were found using Repliset. The crack length determinations from Repliset were nearly the same as that from a direct examination of the slot surface. Further, the Repliset method was able to characterize other damage mechanisms including flaws and scratches on the slot surfaces. In quantitative terms, the Repliset method was able to consistently detect cracks as small as 0.005 inches long and pit-like surface defects as small as 0.001 inches long. Crack detection was more difficult after polishing cracked surfaces, but results show that through-thickness cracks and corner cracks can still be detected, and smaller cracks can be detected after tensile loading is applied to the specimens. Results show that the quality of the surface finish can significantly affect the crack initiation life; high-quality slot surface finished result in higher crack initiation lives than unpolished surfaces by at least a factor of four.

References

1. J. A. Newman, S. W. Smith, S. A. Willard, and R. S. Piascik, "A Comparison of Weld-Repaired and Base Metal for Inconel 718 and CRES 321 at Cryogenic and Room Temperatures," NASA/TM-2004-213253, ARL-TR-3266.
2. J. C. Melcher and D. A. Rigby, "Analysis and Repair of Cracks in the Space Shuttle Main Propulsion System Propellant Feedlines," Proceeding of the 39th AIAA/ASME/SAE/ASEE Joint Propulsion Conference and Exhibit, 20-23 July 2003, Huntsville, Alabama, AIAA 2003-4609.
3. M.H. Swain, R. A. Everett, J.C. Newman, Jr., and E. P. Phillips, "The Growth of Short Cracks in 4340 Steel and Aluminum-Lithium 2090," AGARD Report No. 767, Short-Crack Growth Behaviour in Various Aircraft Materials, August 1990, Advisory Group for Aerospace Research and Development.
4. *Small-crack Test Methods*, J.M. Larsen and J.E. Allison, Eds., *ASTM STP 1149*, American Society for Testing and Materials, Philadelphia, PA, 1992.
5. N.E. Dowling, *Mechanical Behavior of Materials: Engineering Methods for Deformation, Fracture, and Fatigue*, Prentice Hall, Upper Saddle River, NJ, 1999.
6. *Small Fatigue Cracks*, R.O. Ritchie and J. Lankford, Eds., American Institute of Mining and Metallurgical Engineers, Warrendale, PA, 1986.
7. *Mechanics of Fatigue Crack Closure*, J.C. Newman, Jr. and W. Elber, Eds., ASTM STP 982, American Society for Testing and Materials, Philadelphia, PA, 1988.

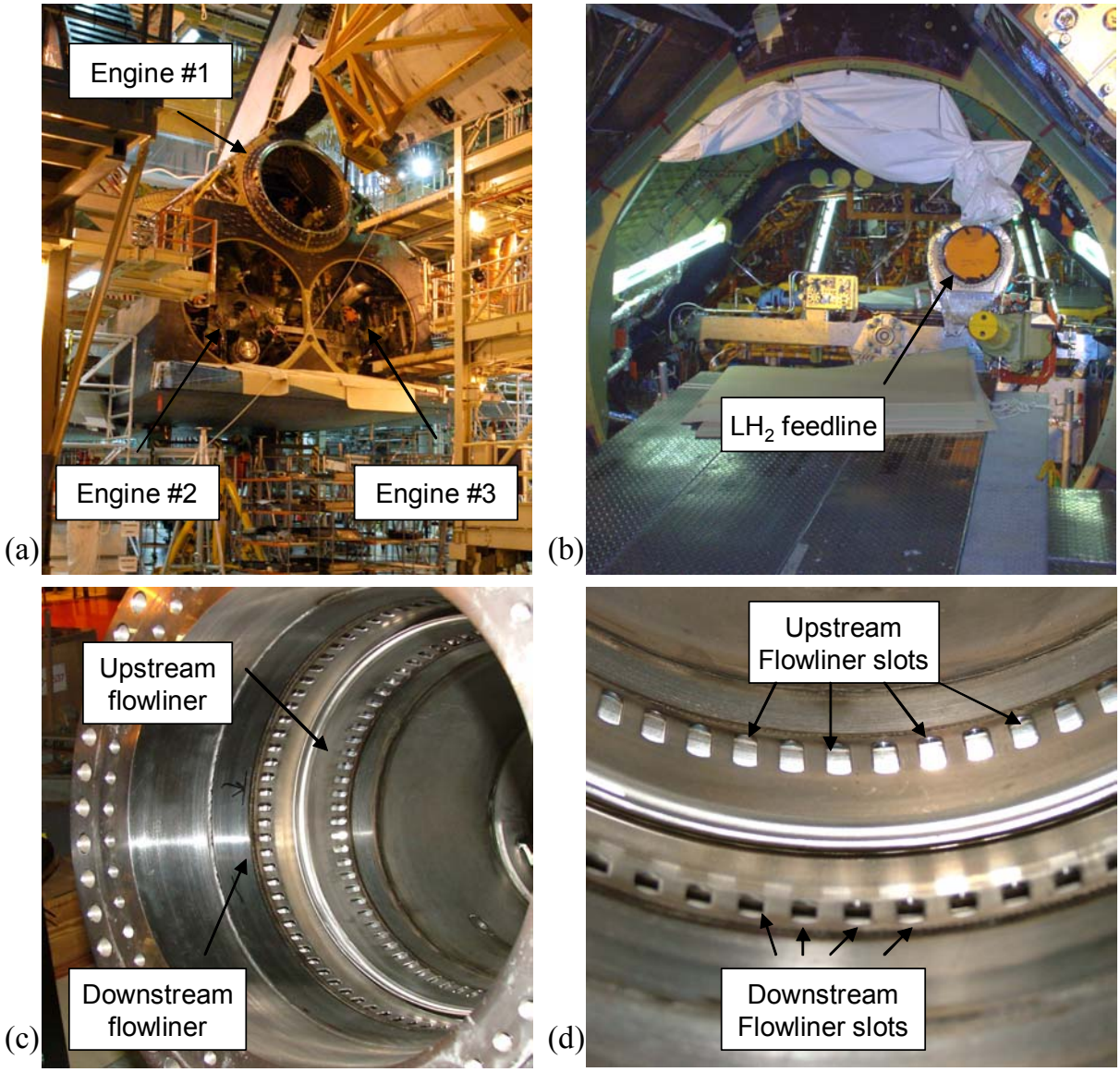

Figure 1. The flowliner locations on the space shuttle orbiter are shown in a series of photographs. (a) Orbiter aft end shown with main engines removed. (b) LH_2 feedline is shown in the main engine orifice. (c) Flowliners are shown inside the LH_2 feedline. (d) Flowliner slots.

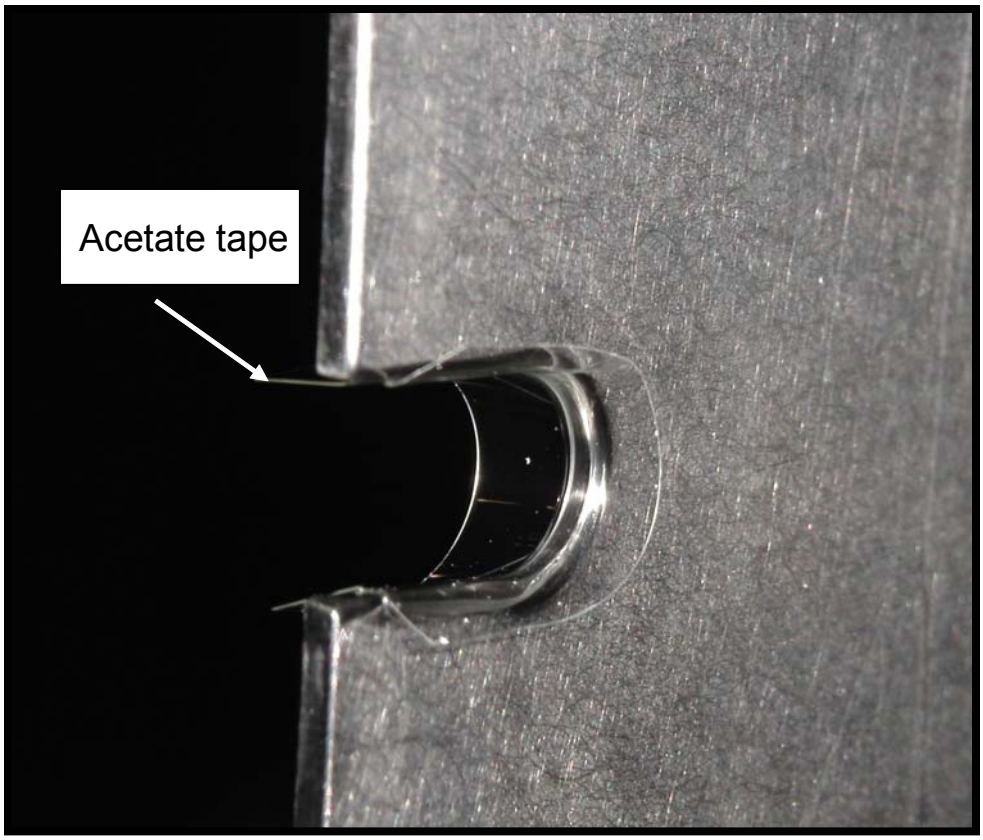

Figure 2. Photograph of acetate tape replication method.

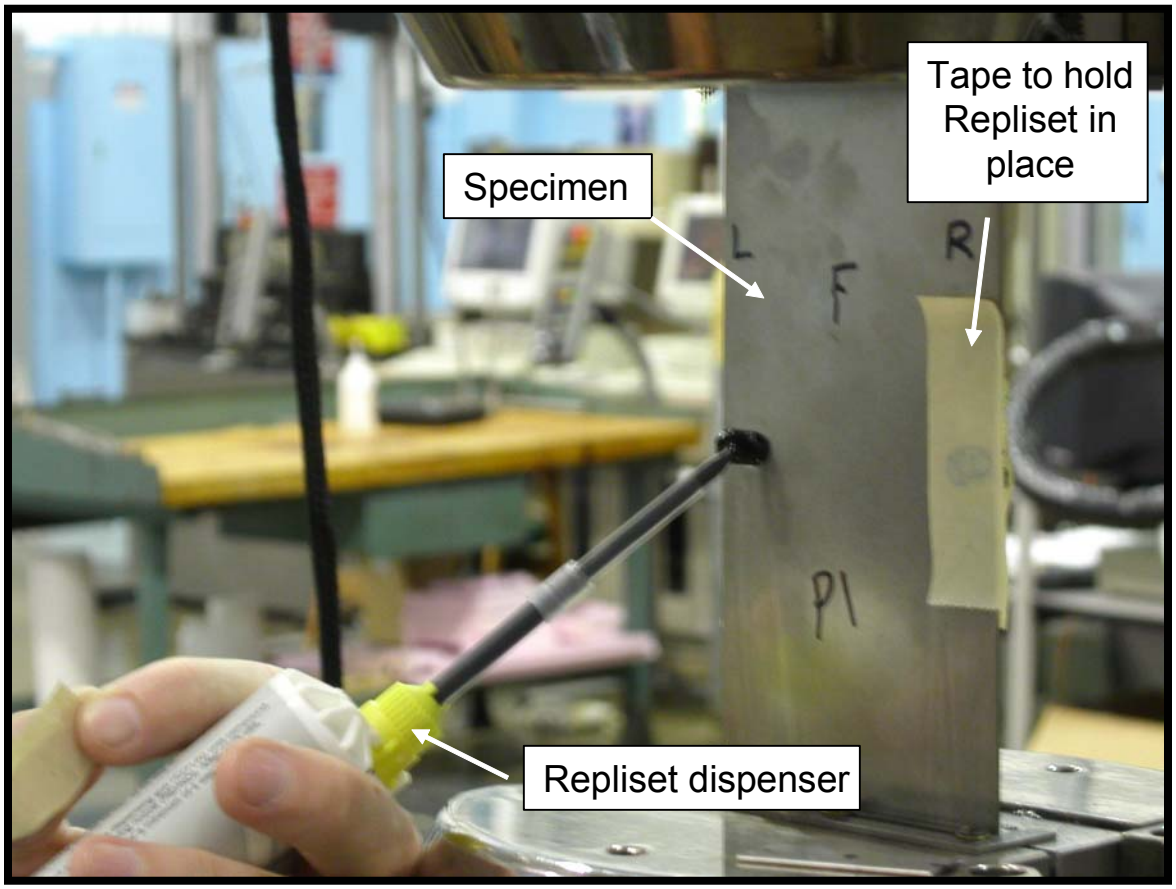

Figure 3. Photograph of Repliset applied to a double-edge notch specimen.

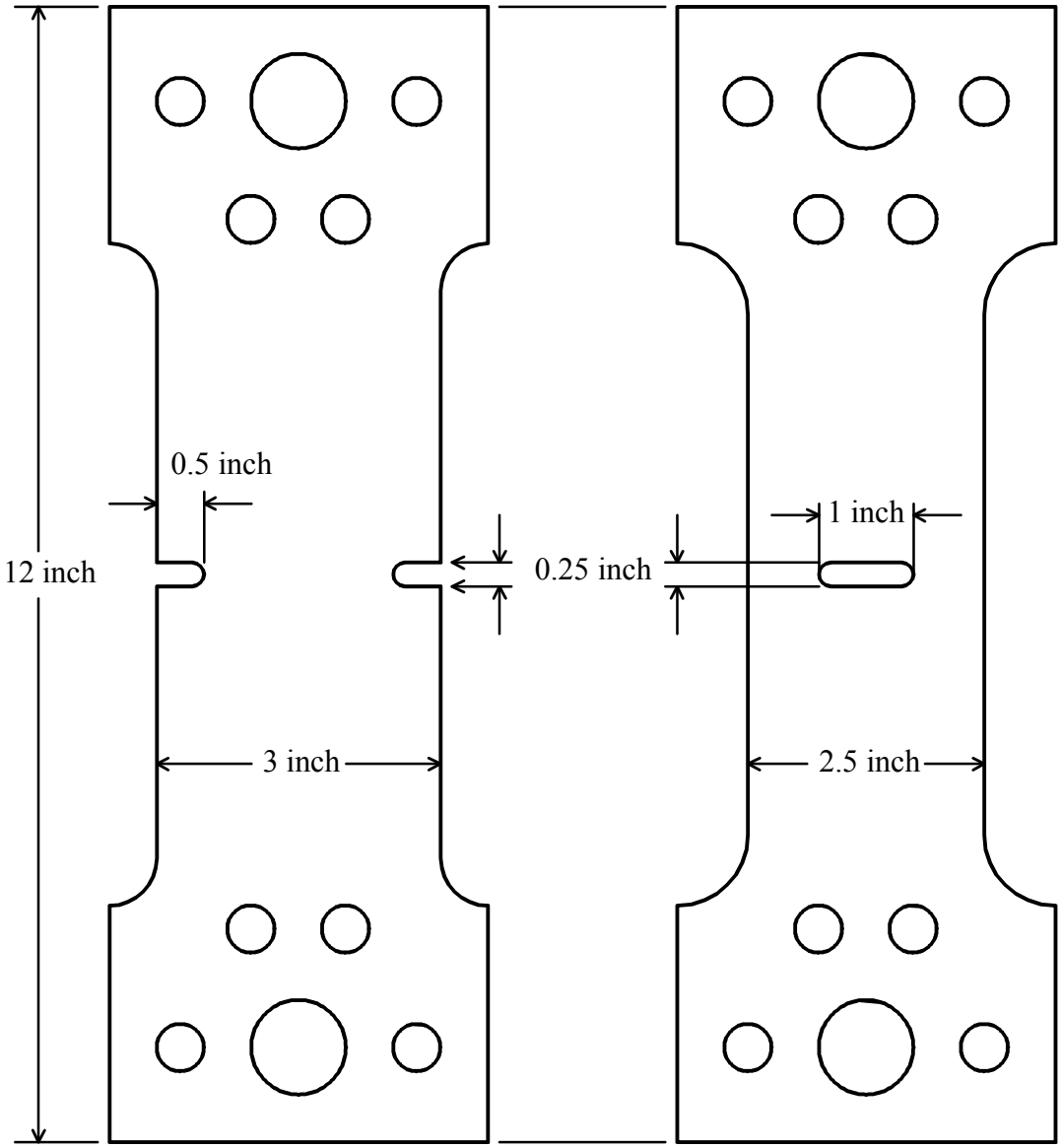

Figure 4. Drawings of the slotted specimen configurations used in this study. (a) Double-edge notch specimen. (b) Center-slot specimen.

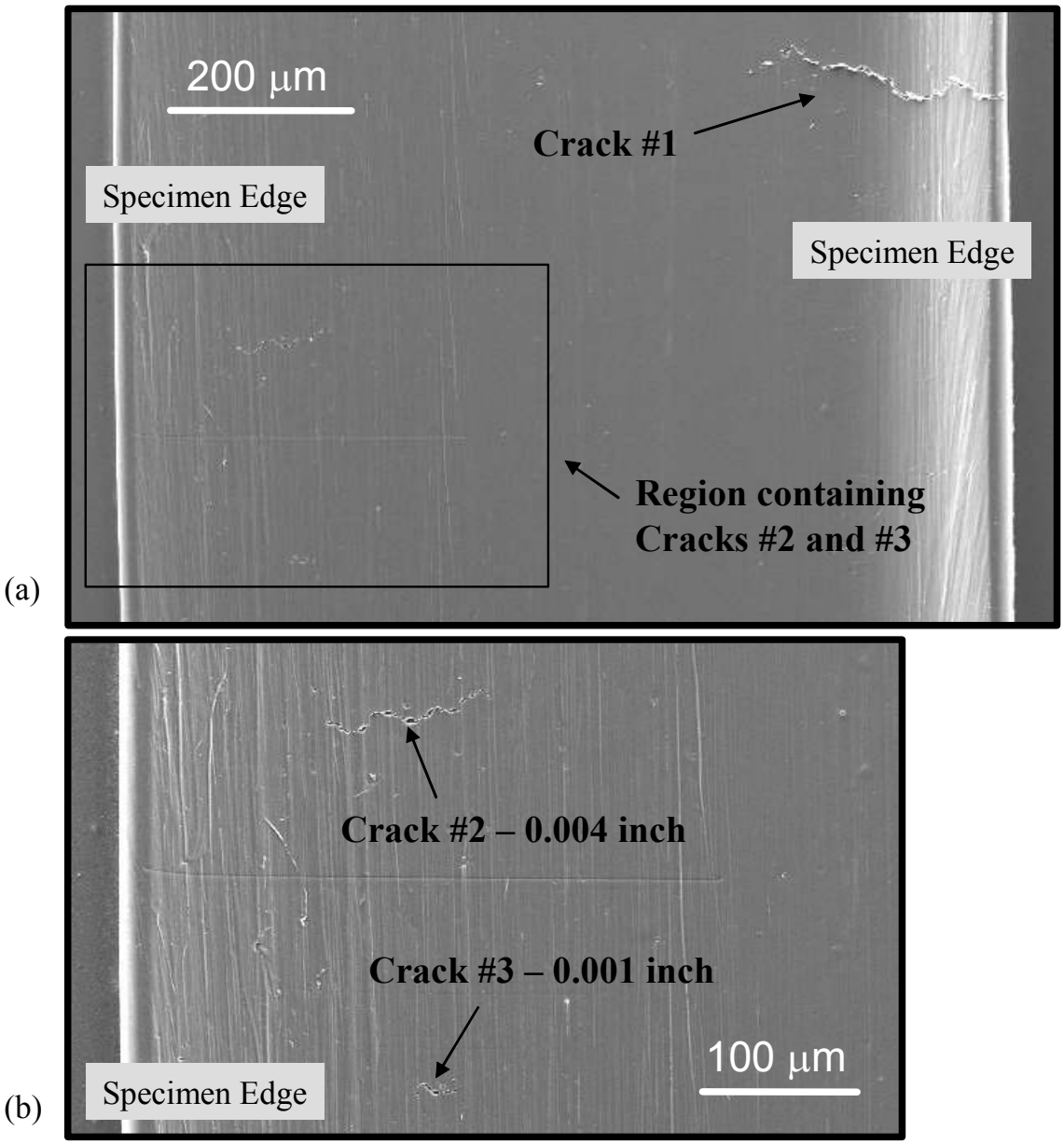

Figure 5. SEM images of specimen P1 acetate tape replica. (a) Low magnification. (b) High magnification of region containing cracks #2 and #3.

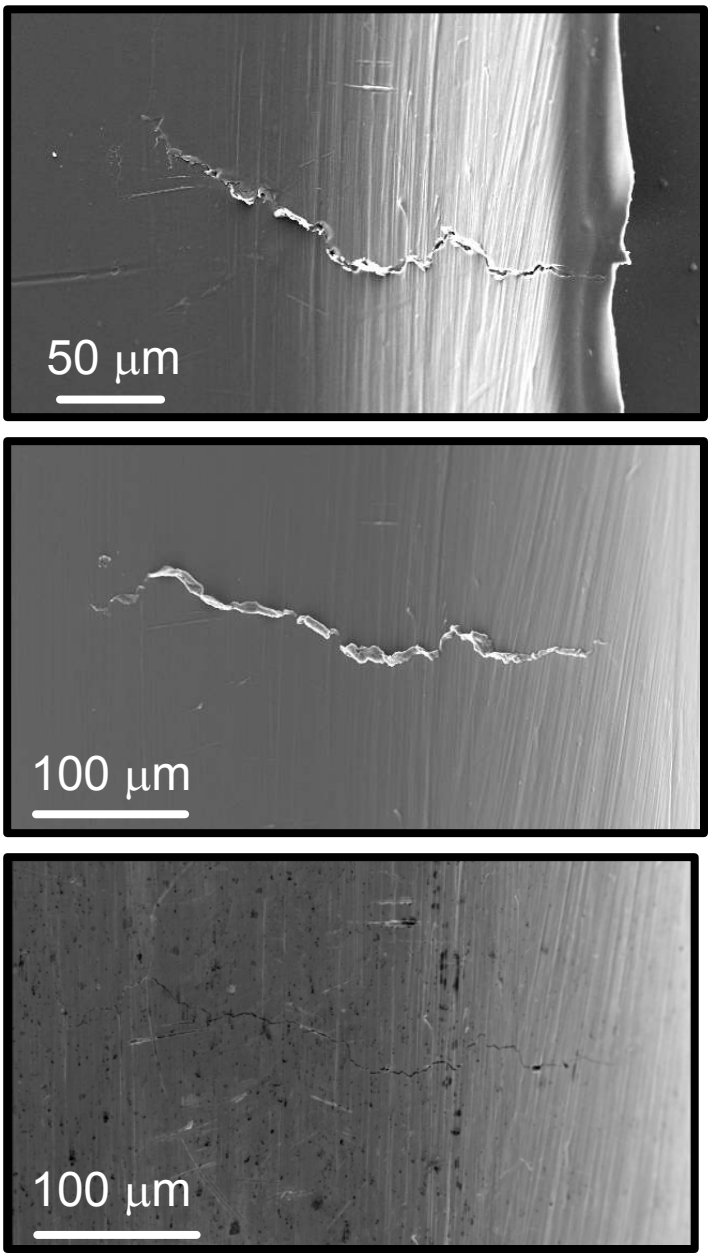

Figure 6. SEM images of crack #1 on specimen P1, a 0.012-inch-long corner crack. (a) Acetate tape replica (maximum load). (b) Repliset replica (unloaded). (c) Specimen (unloaded).

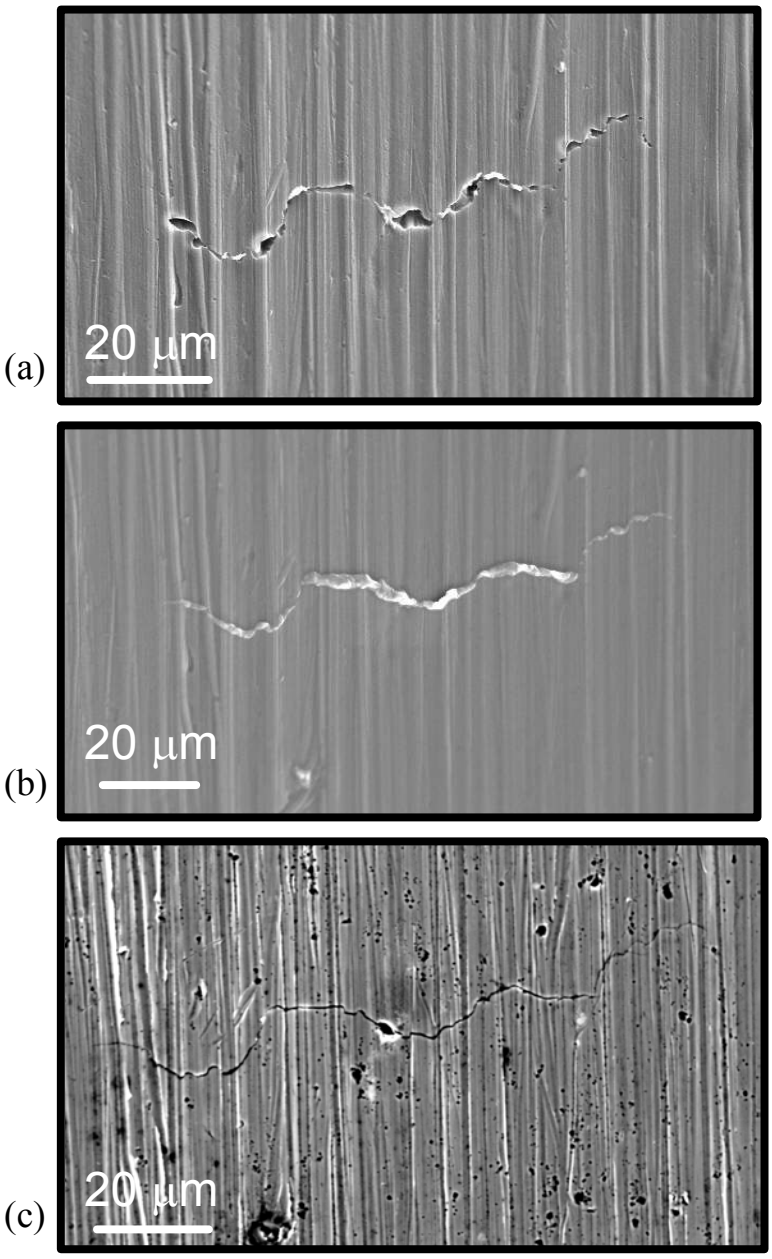

Figure 7. SEM images of crack #2 on specimen P1, a 0.004-inch-long surface crack. (a) Acetate tape replica (maximum load). (b) Repliset replica (unloaded). (c) Specimen (unloaded).

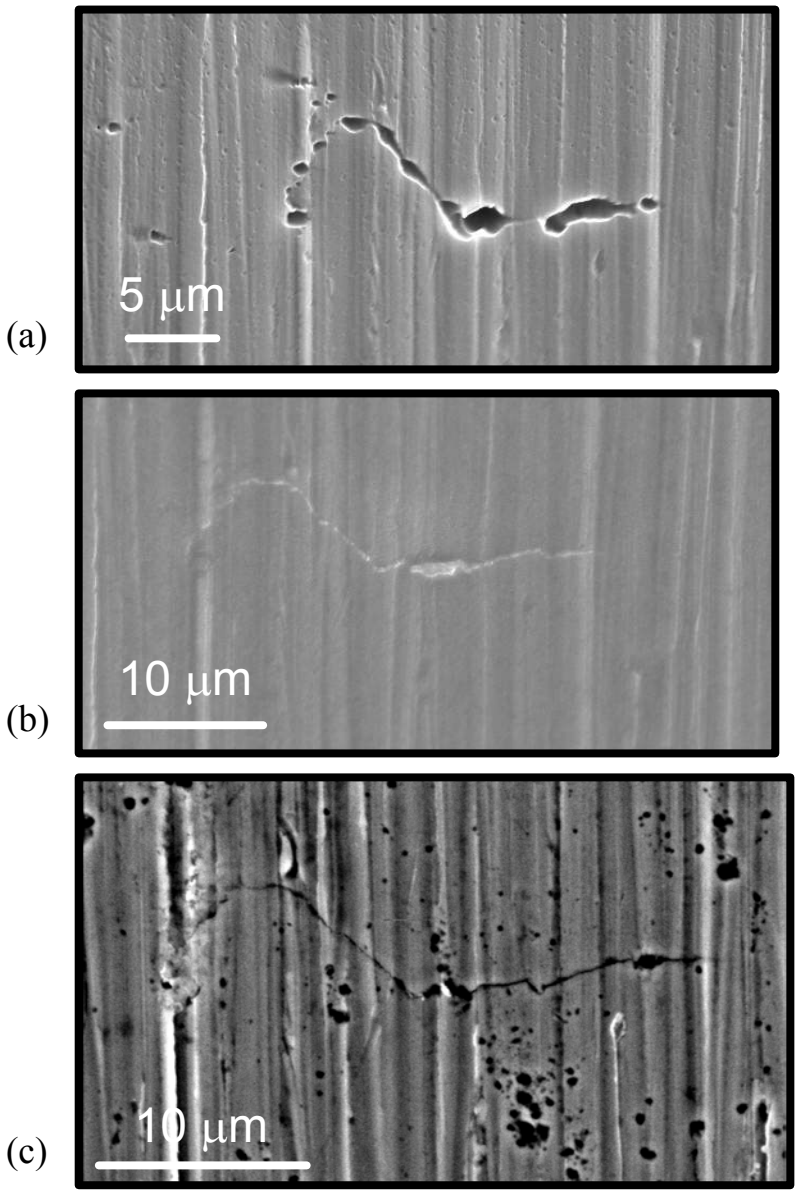

Figure 8. SEM images of crack #3 on specimen P1, a 0.001-inch-long surface crack. (a) Acetate tape replica (maximum load). (b) Repliset replica (unloaded). (c) Specimen (unloaded).

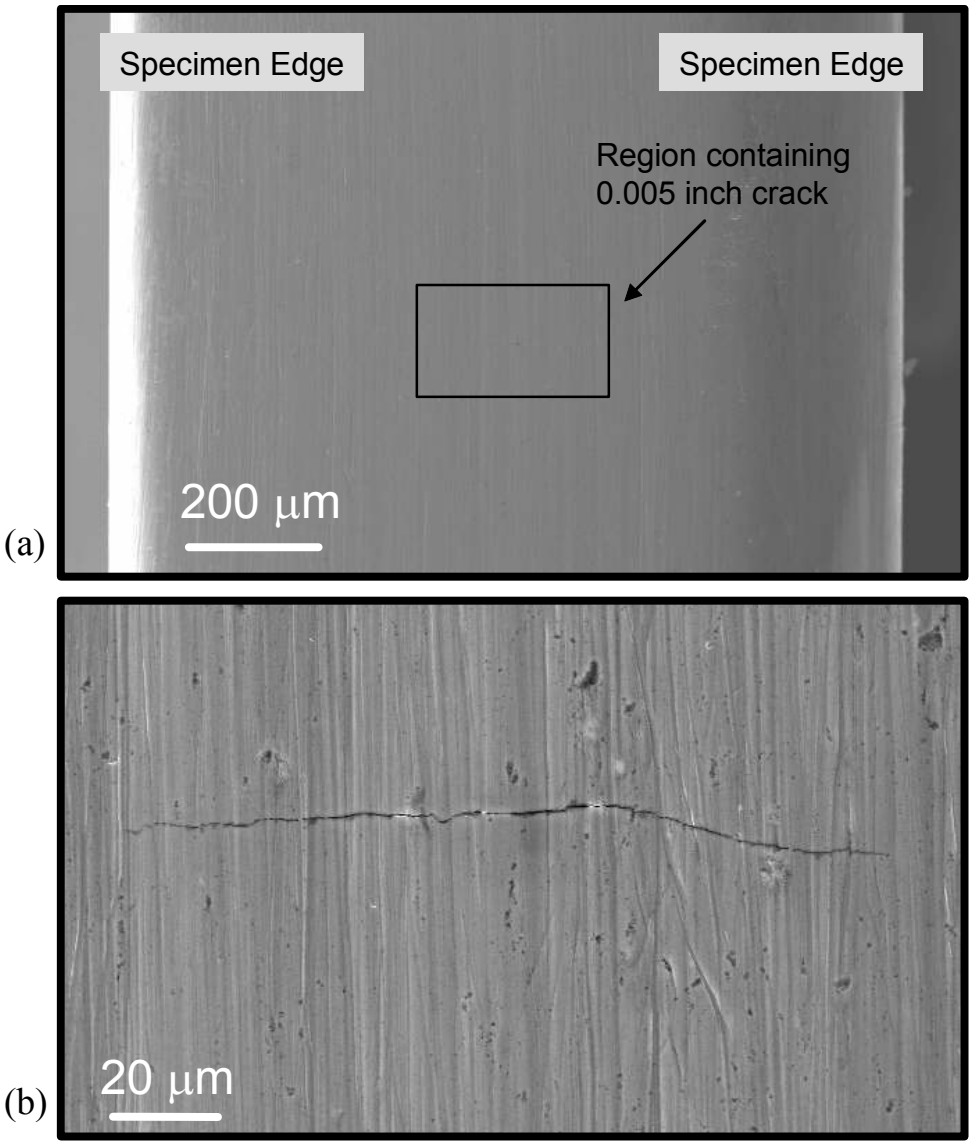

Figure 9. SEM images of specimen P2 acetate tape replica. (a) Low magnification. (b) High magnification of the region containing a 0.005-inch-long surface crack.

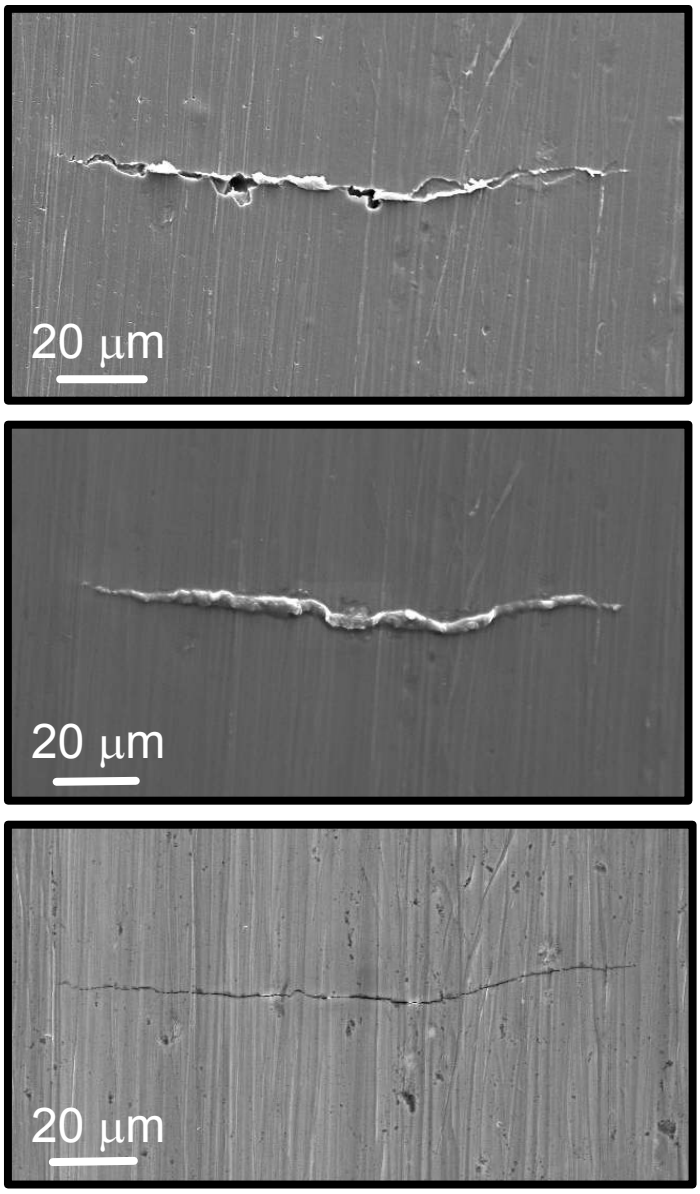

Figure 10. SEM images of the 0.005-inch-long surface crack on specimen P2. (a) Acetate tape replica (maximum load). (b) Repliset replica (unloaded). (c) Specimen (unloaded).

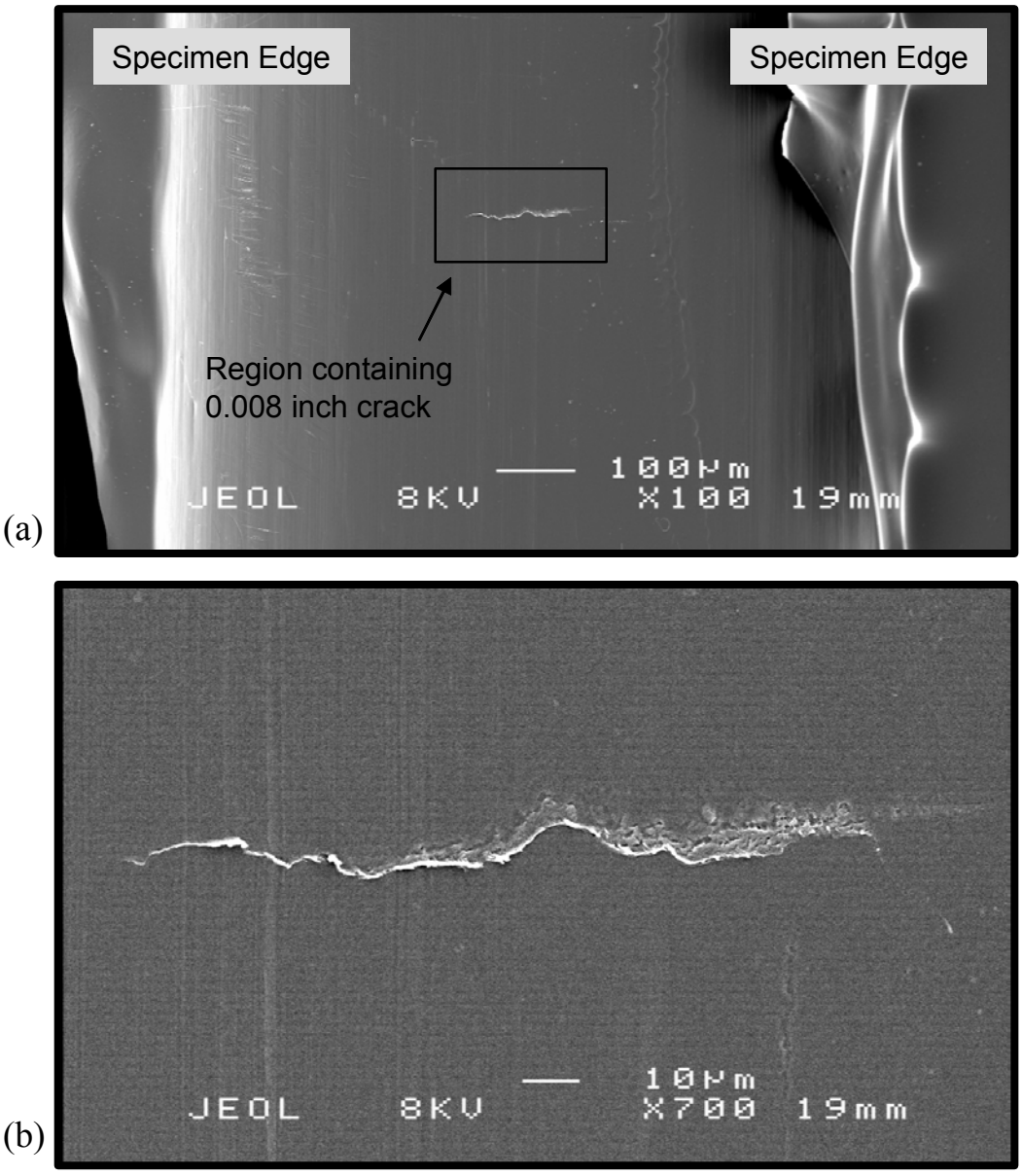

Figure 11. SEM images of specimen C3 acetate tape replica. (a) Low magnification. (b) High magnification of the region containing a 0.008-inch-long surface crack.

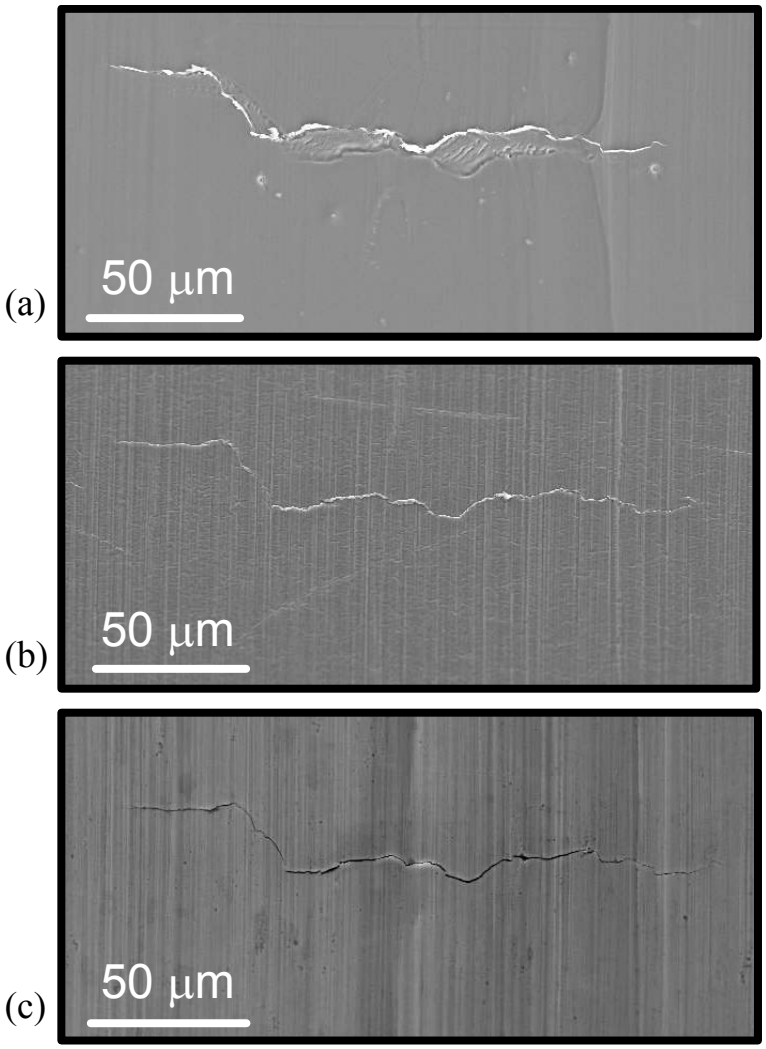

Figure 12. SEM images of the 0.008-inch-long surface crack on specimen C3. (a) Acetate tape replica (maximum load). (b) Repliset replica (unloaded). (c) Specimen (unloaded).

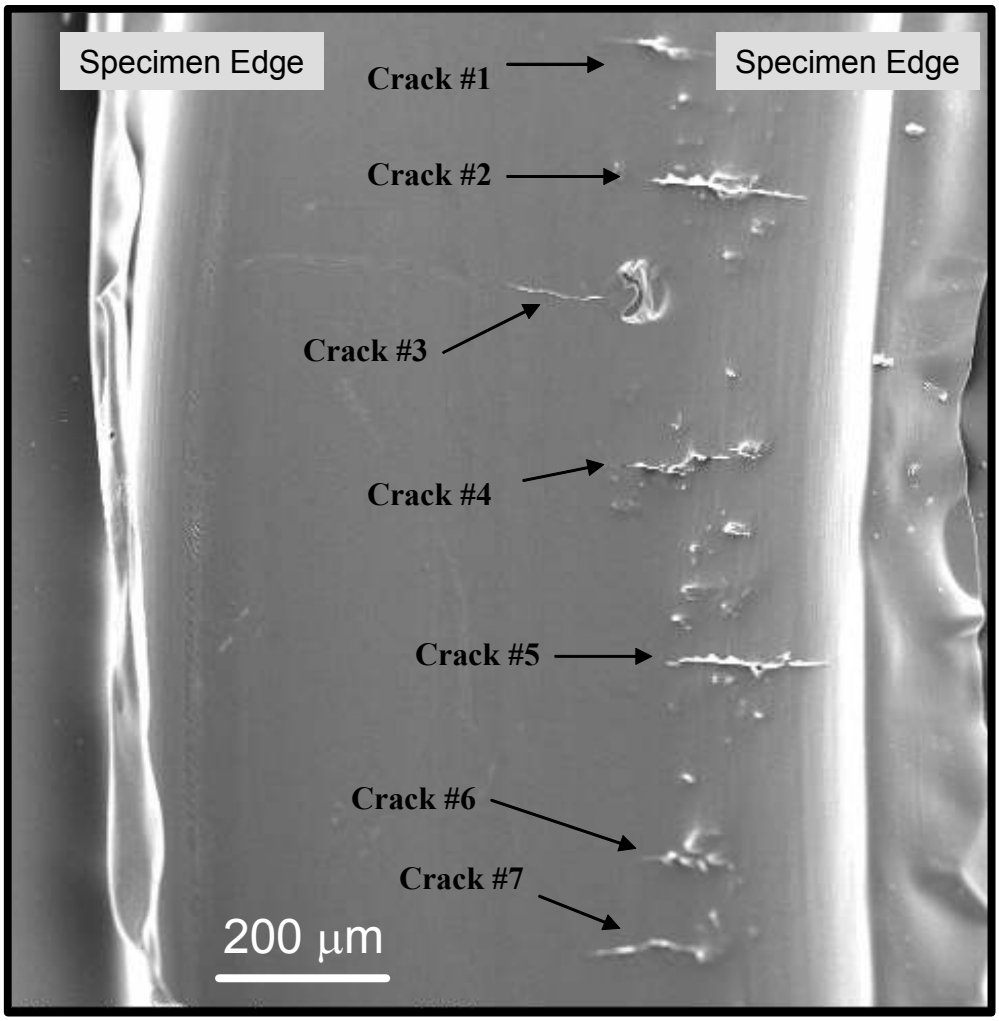

Figure 13. SEM image of specimen C6 acetate tape replica.

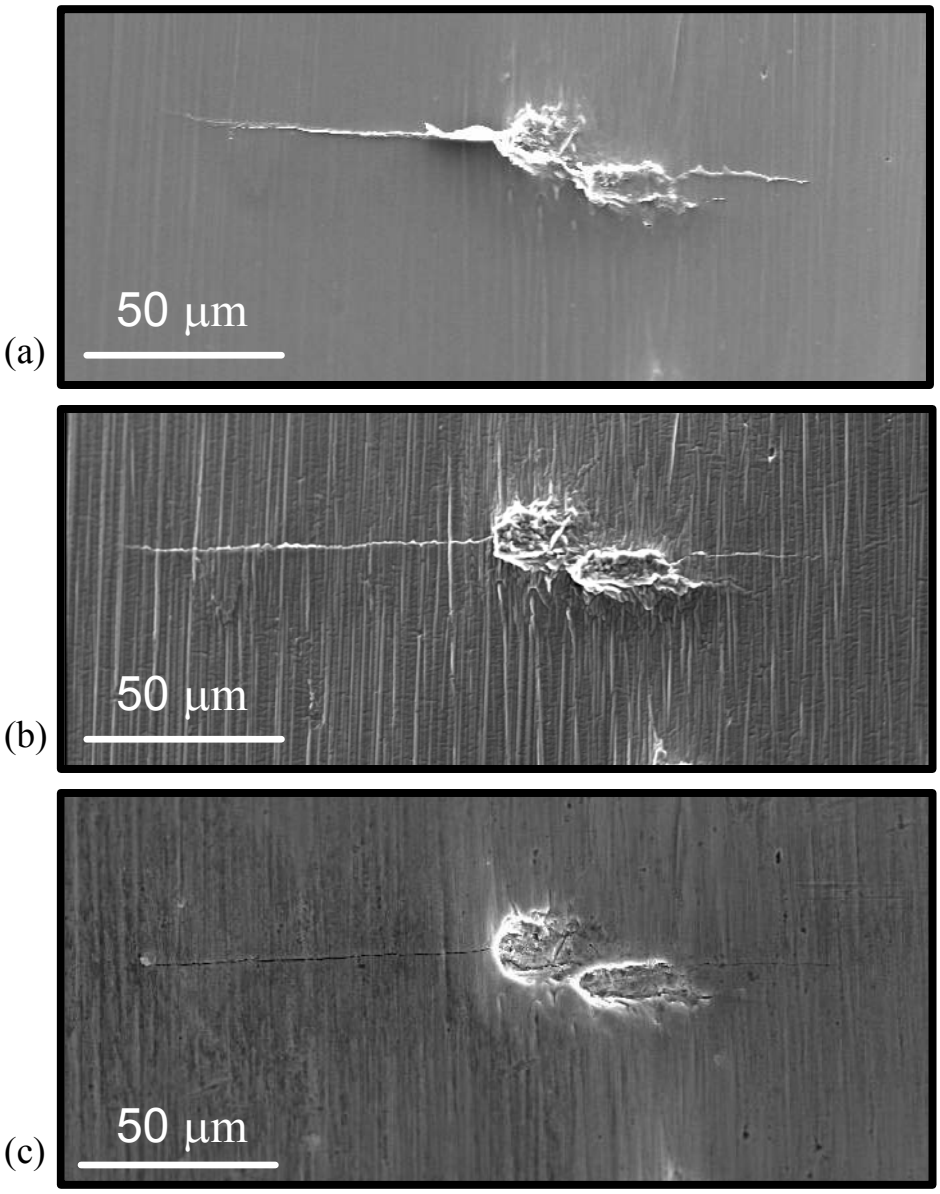

Figure 14. SEM images of crack #1 on specimen C6, a 0.006-inch-long surface crack. (a) Acetate tape replica (maximum load). (b) Repliset replica (unloaded). (c) Specimen (unloaded).

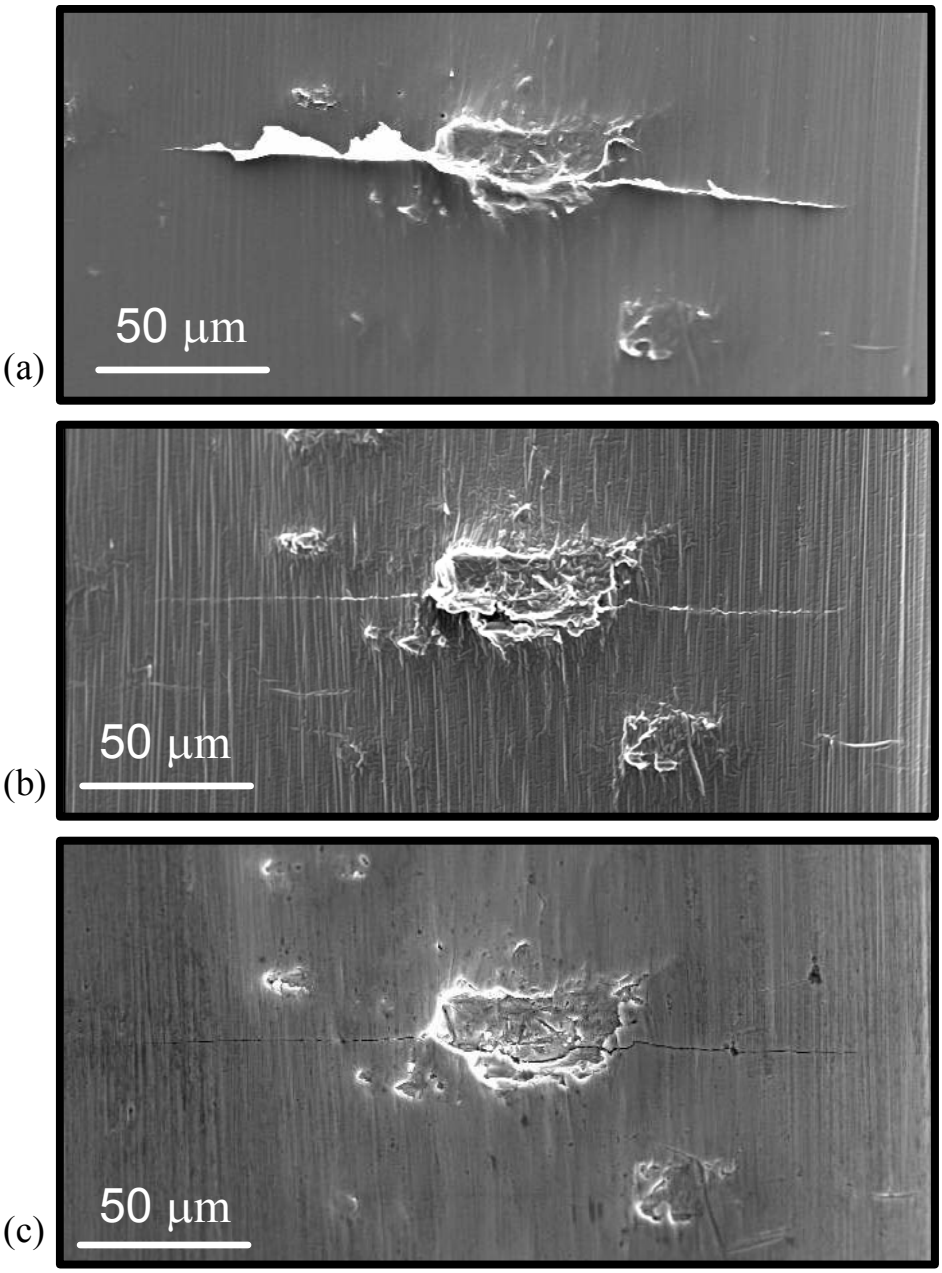

Figure 15. SEM images of crack #2 on specimen C6, a 0.008-inch-long surface crack. (a) Acetate tape replica (maximum load). (b) Repliset replica (unloaded). (c) Specimen (unloaded).

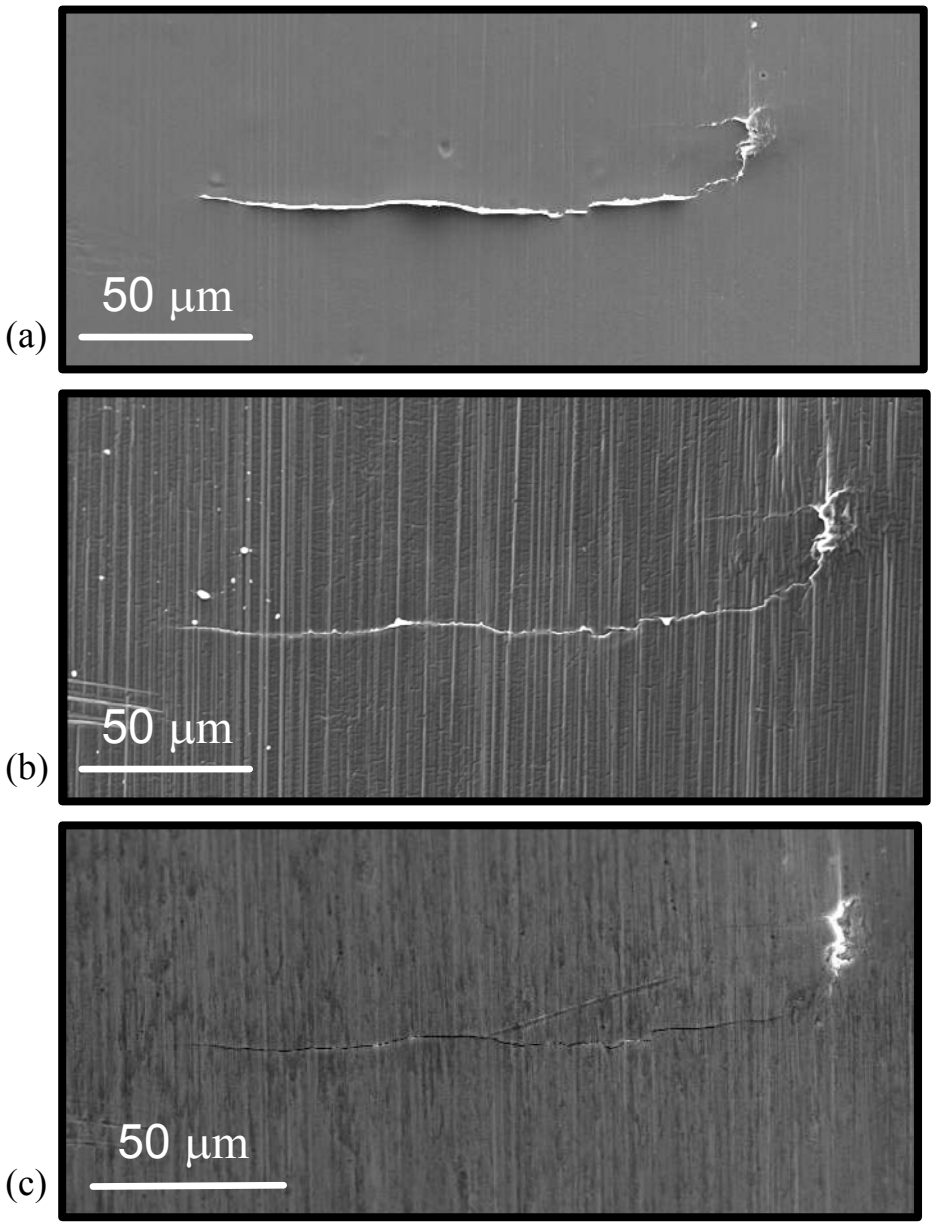

Figure 16. SEM images of crack #3 on specimen C6, a 0.007-inch-long surface crack. (a) Acetate tape replica (maximum load). (b) Repliset replica (unloaded). (c) Specimen (unloaded).

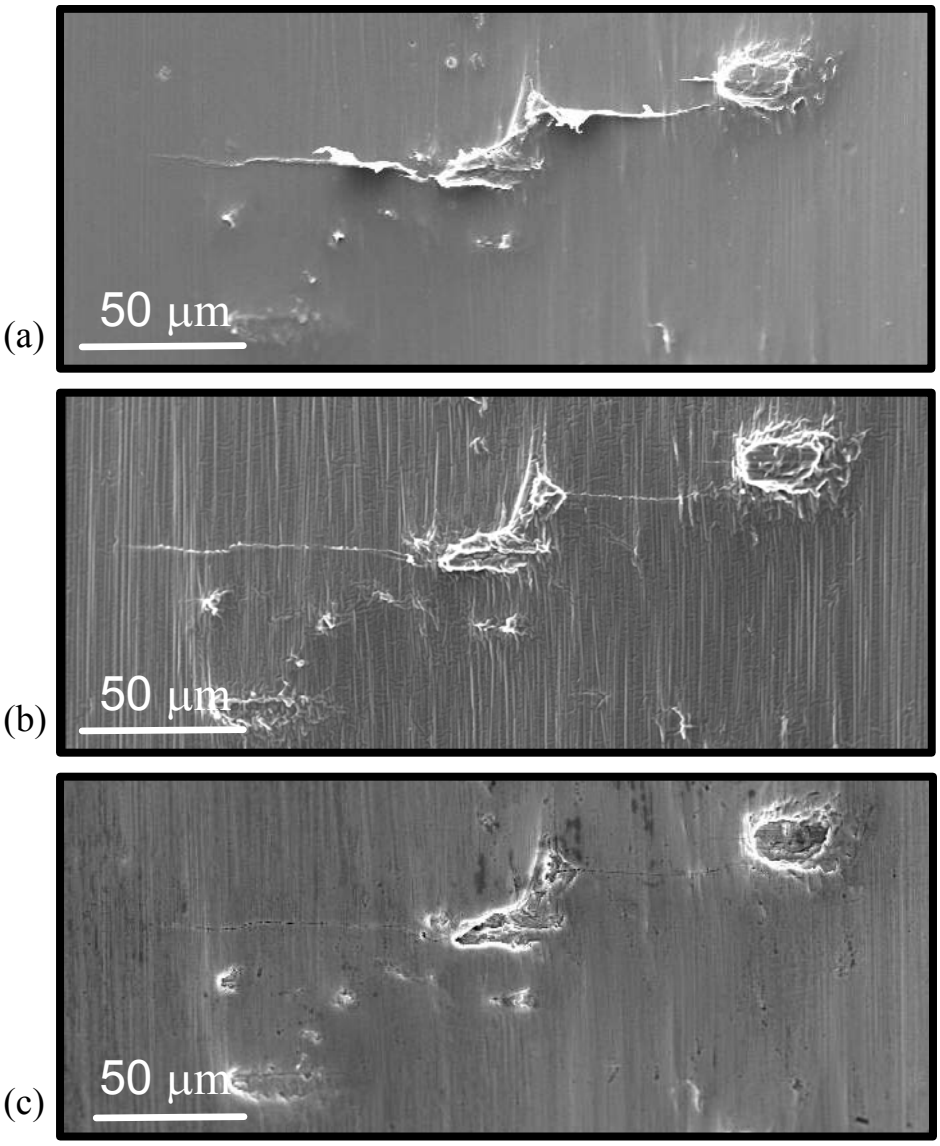

Figure 17. SEM images of crack #4 on specimen C6, a 0.008-inch-long surface crack. (a) Acetate tape replica (maximum load). (b) Repliset replica (unloaded). (c) Specimen (unloaded).

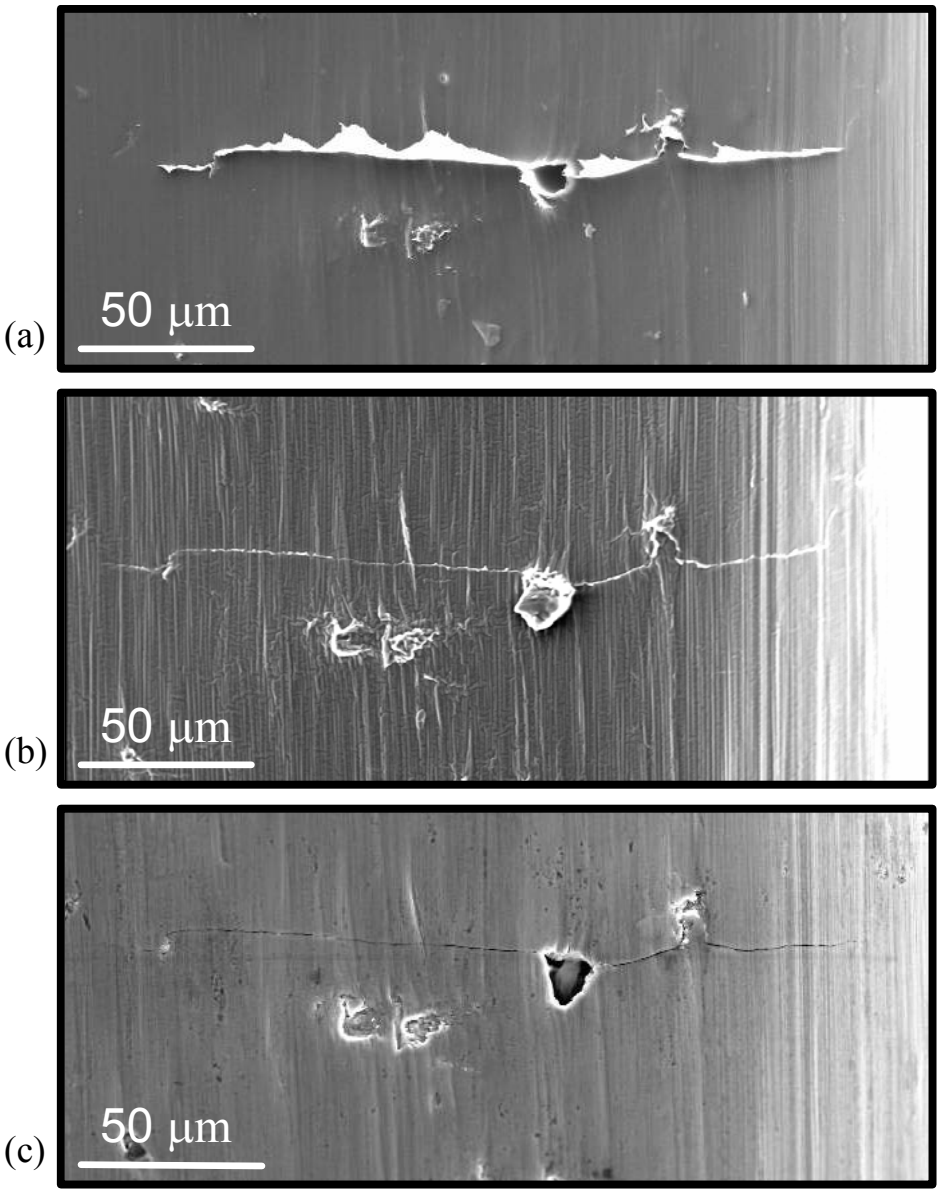

Figure 18. SEM images of crack #5 on specimen C6, a 0.008-inch-long surface crack. (a) Acetate tape replica (maximum load). (b) Repliset replica (unloaded). (c) Specimen (unloaded).

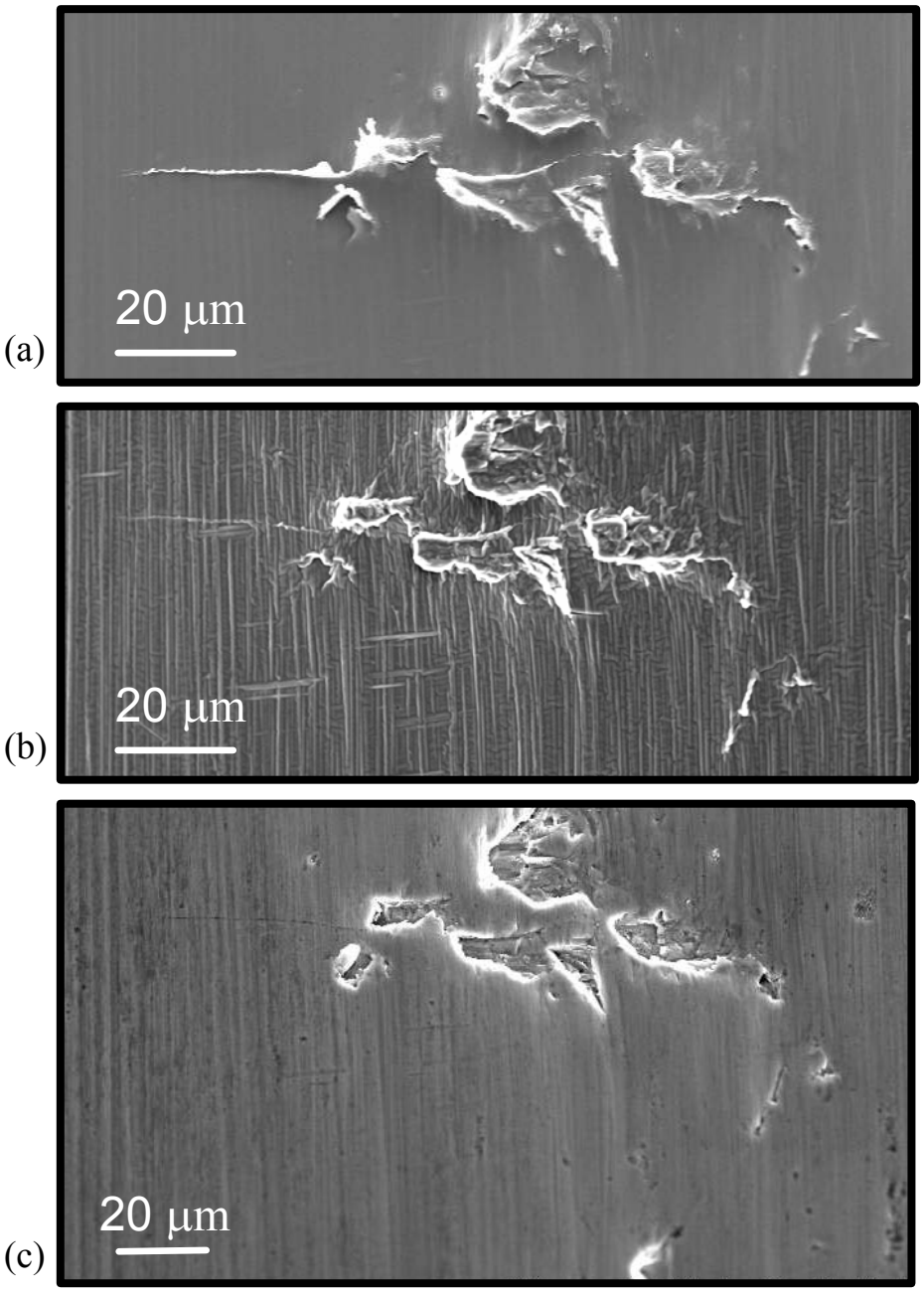

Figure 19. SEM images of crack #6 on specimen C6, a 0.002-inch-long surface crack. (a) Acetate tape replica (maximum load). (b) Repliset replica (unloaded). (c) Specimen (unloaded).

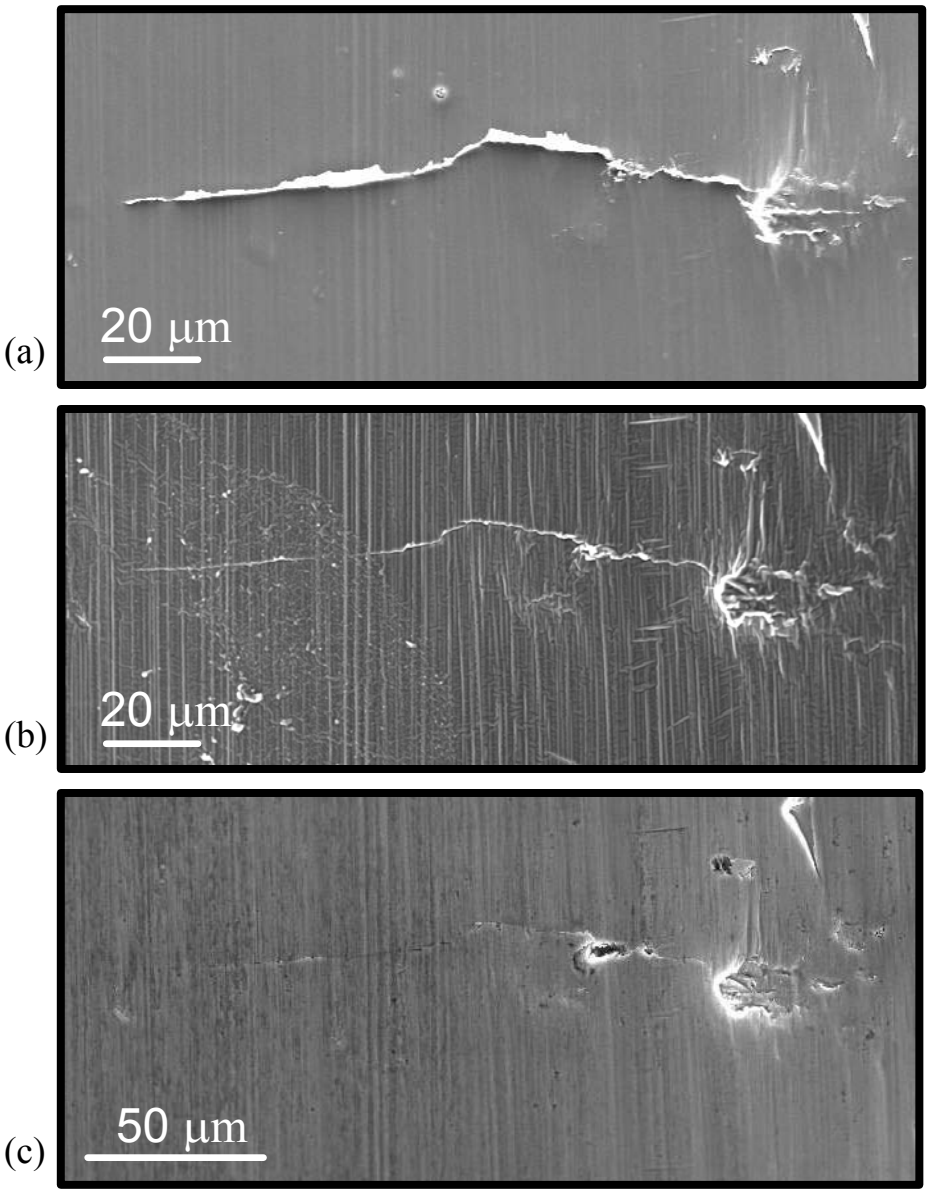

Figure 20. SEM images of crack #7 on specimen C6, a 0.006-inch-long surface crack. (a) Acetate tape replica (maximum load). (b) Repliset replica (unloaded). (c) Specimen (unloaded).

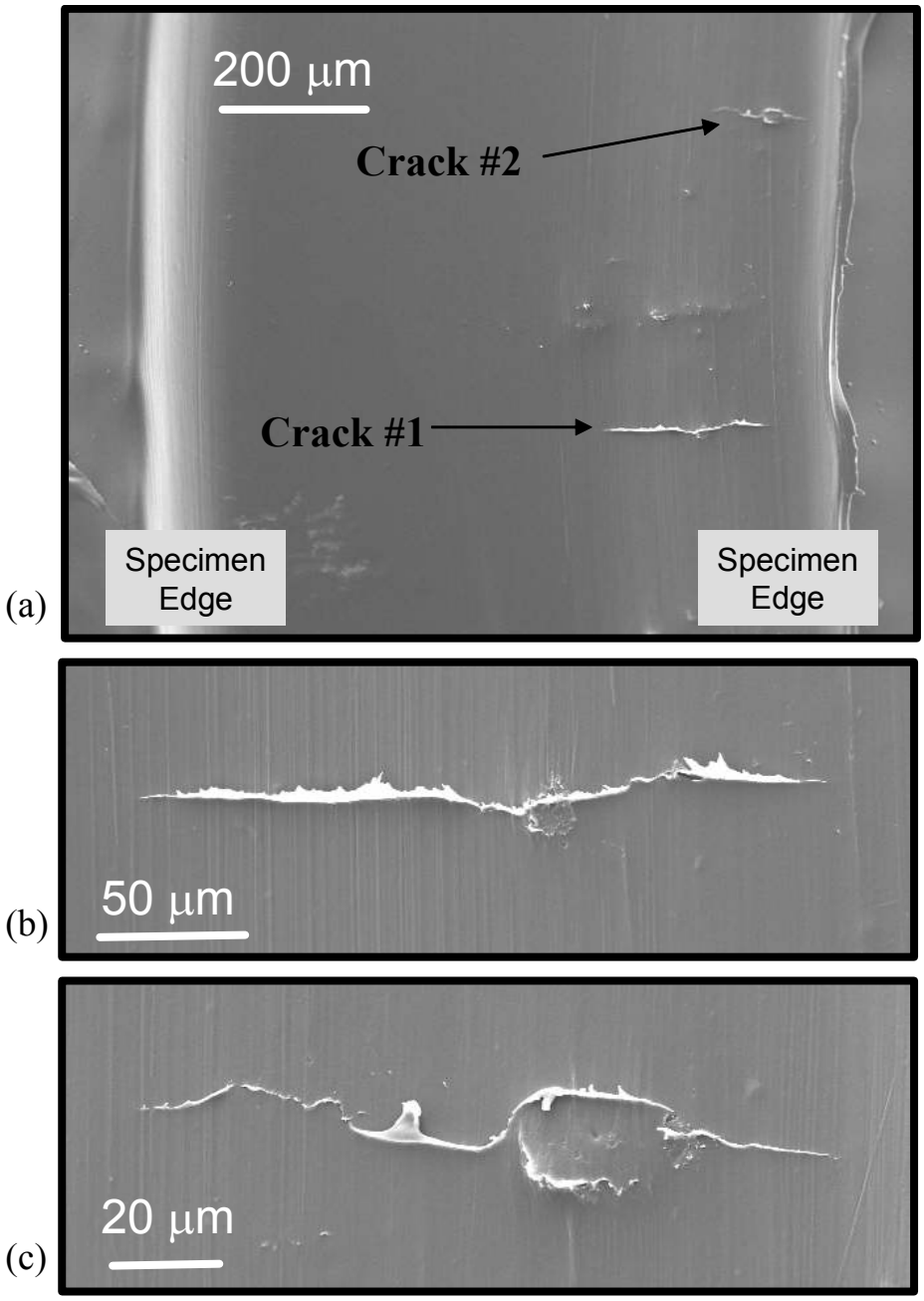

Figure 21. SEM images of specimen C8. (a) Low magnification. (b) High magnification of crack #1, a 0.008-inch-long surface crack. (c) High magnification of crack #2, a 0.005-inch-long surface crack.

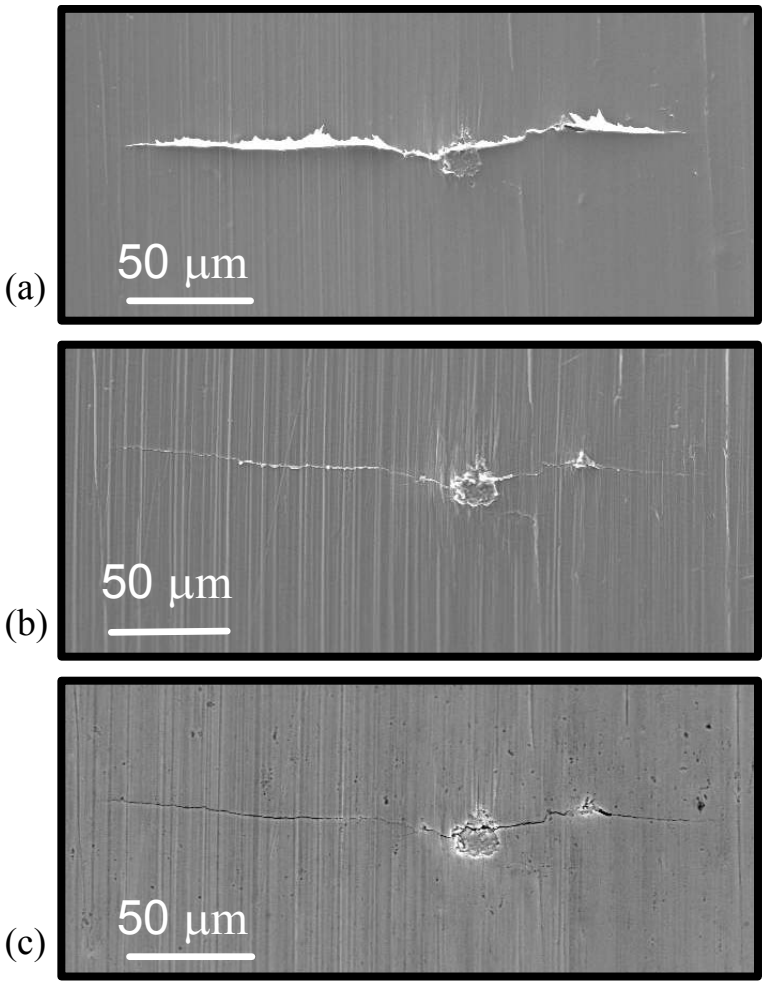

Figure 22. SEM images of crack #1 on specimen C8, a 0.008-inch-long surface crack. (a) Acetate tape replica (maximum load). (b) Repliset replica (unloaded). (c) Specimen (unloaded).

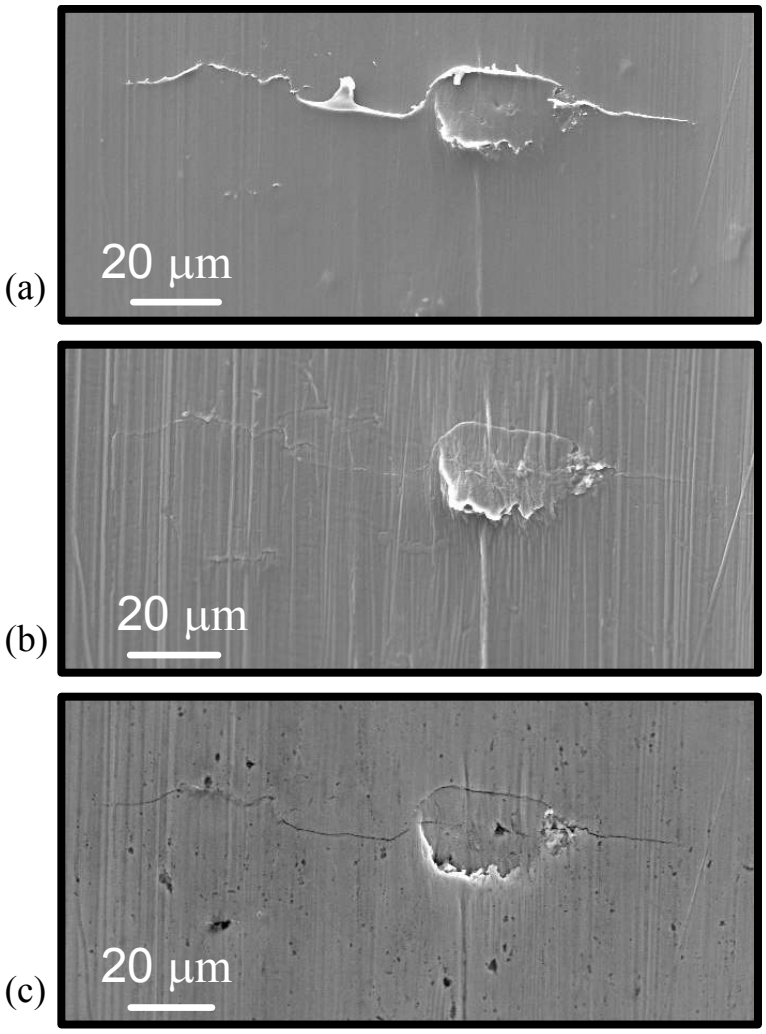

Figure 23. SEM images of crack #2 on specimen C8, a 0.005-inch-long surface crack. (a) Acetate tape replica (maximum load). (b) Repliset replica (unloaded). (c) Specimen (unloaded).

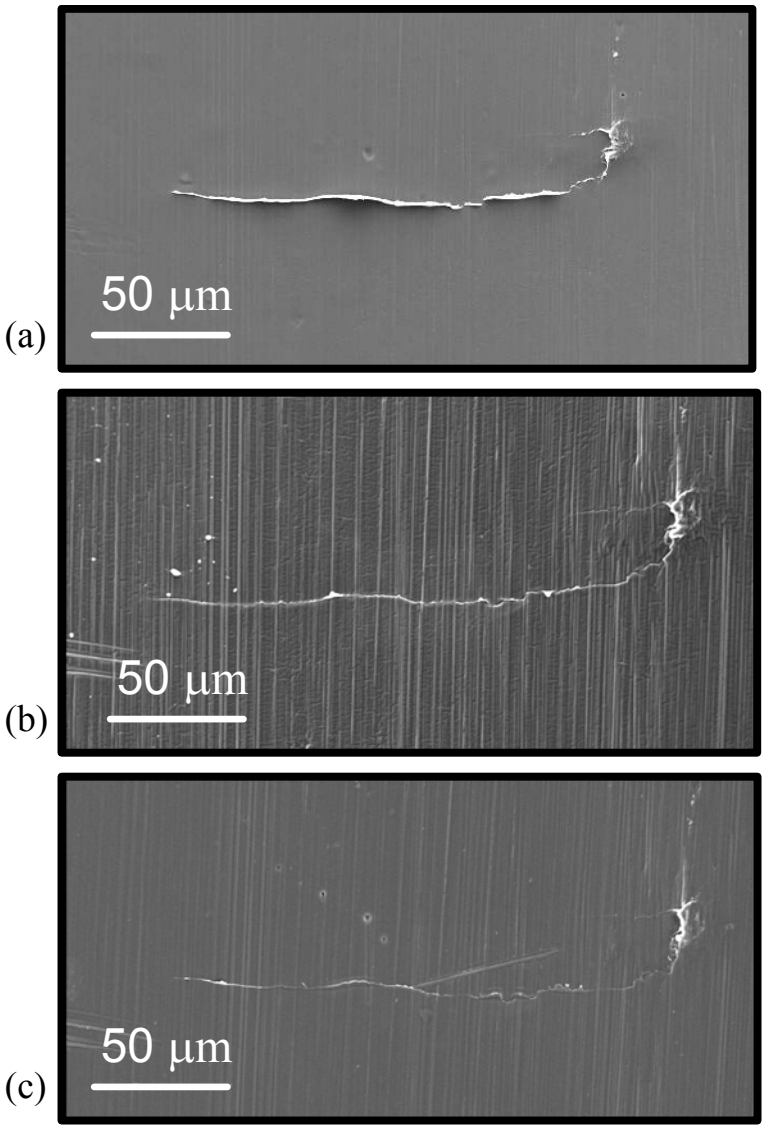

Figure 24. SEM images of crack #3 on specimen C6. (a) Acetate tape replica. (b) First Repliset replica. (c) Fifth Repliset replica.

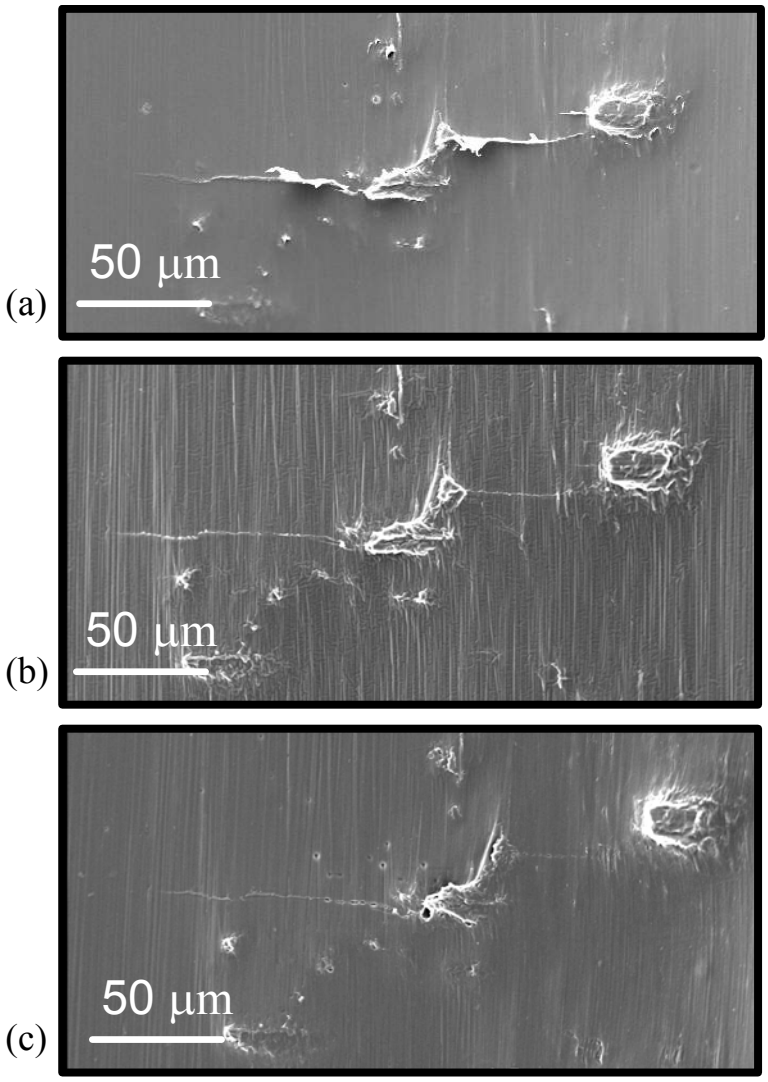

Figure 25. SEM images of crack #4 on specimen C6. (a) Acetate tape replica. (b) First Repliset replica. (c) Fifth Repliset replica.

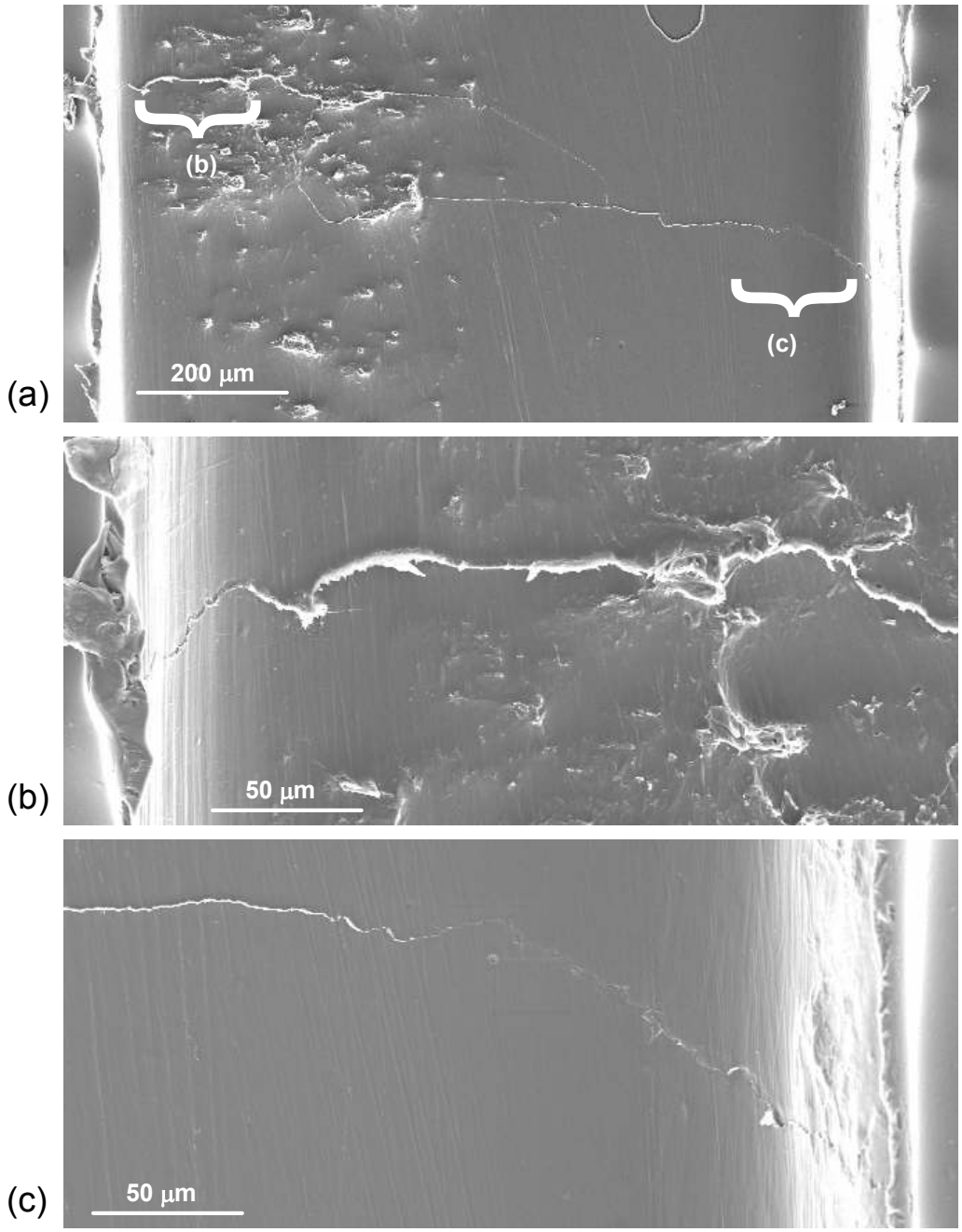

Figure 26. SEM images of specimen C1 before polishing (unloaded). (a) Low magnification. (b) High magnification image of region (b). (c) High magnification image of region (c).

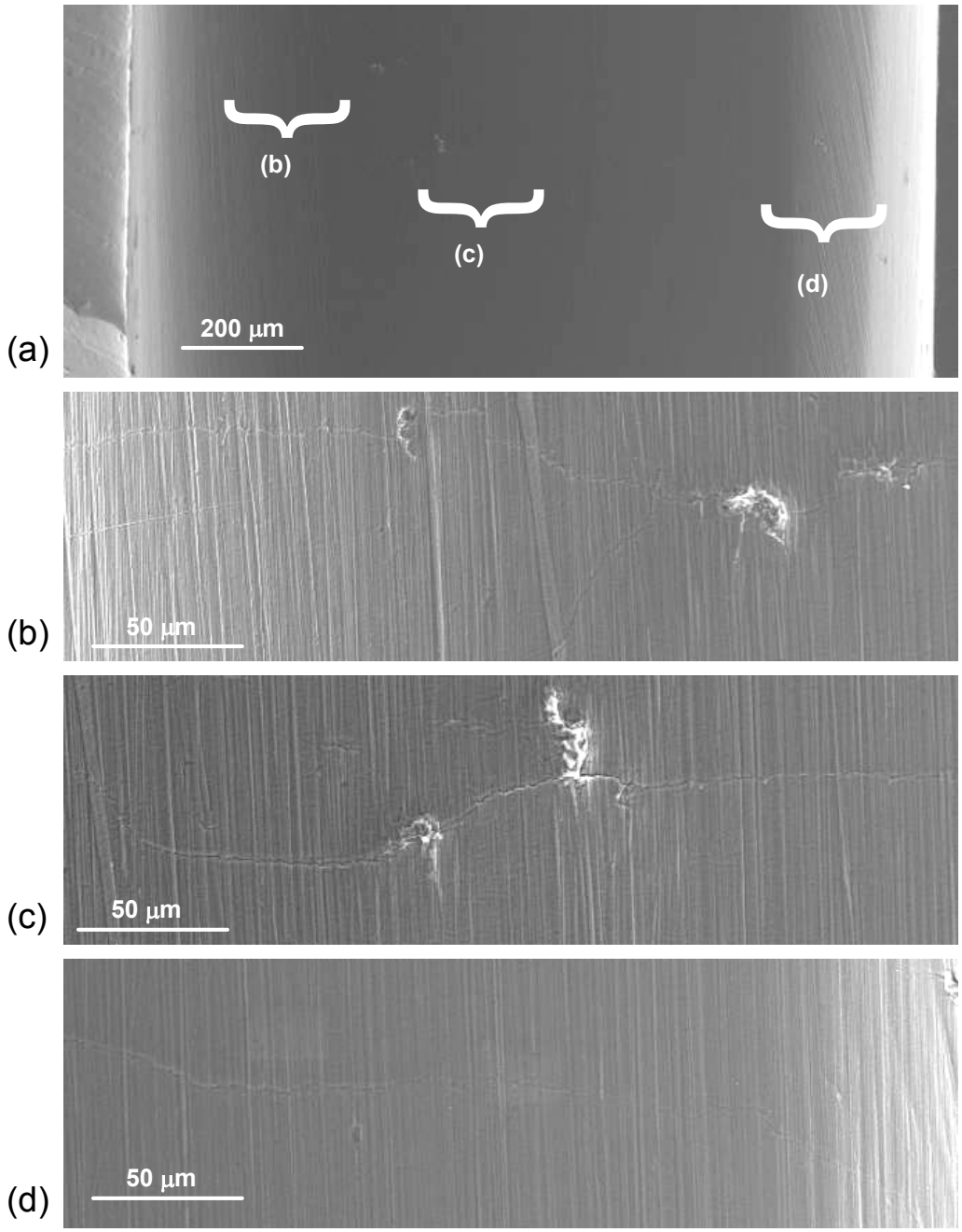

Figure 27. SEM images of specimen C1 after polishing (unloaded). (a) Low magnification. (b) High magnification image of region (b). (c) High magnification image of region (c). (d) High magnification of region (d).

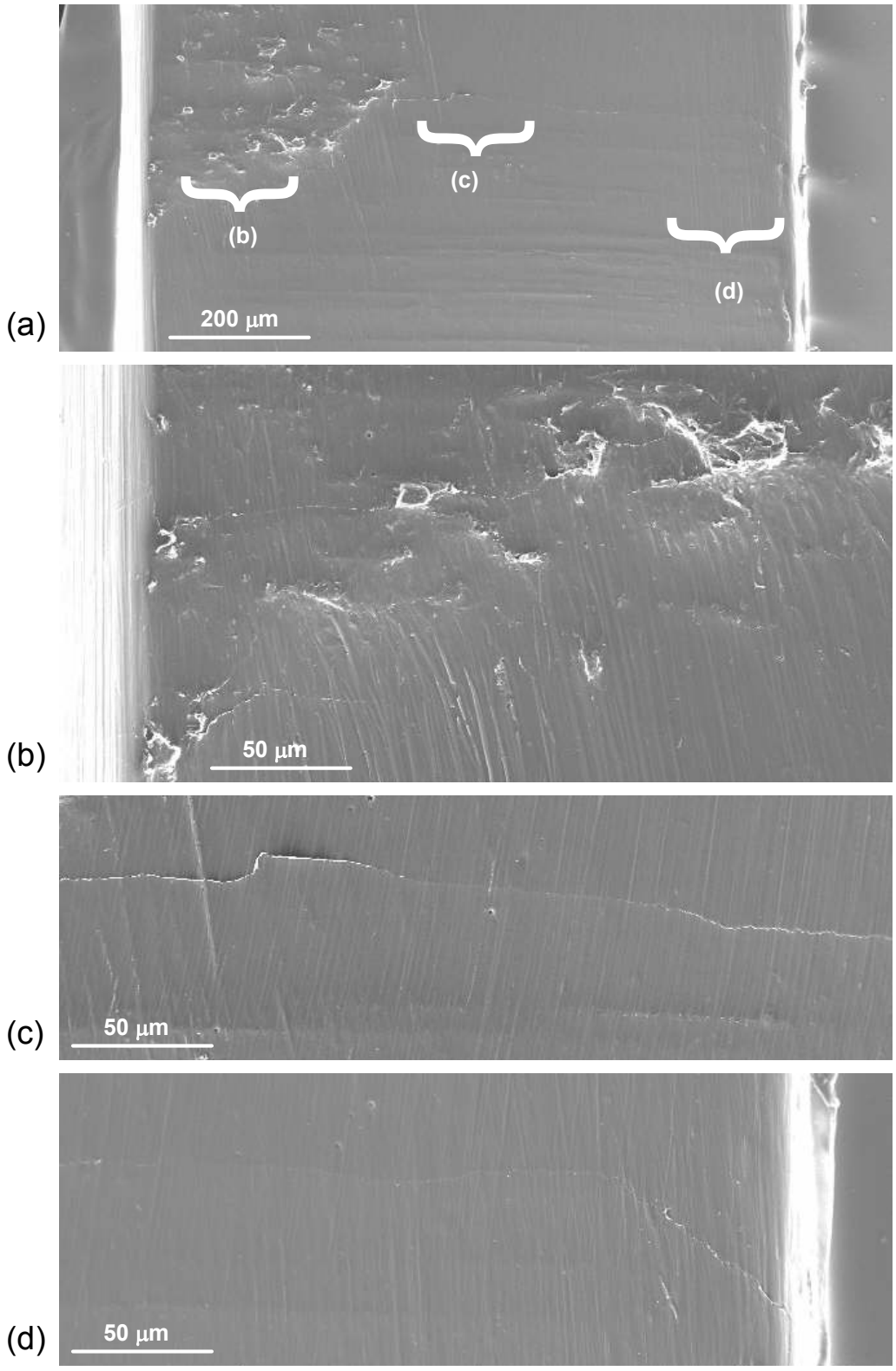

Figure 28. SEM images of specimen C2 before polishing (unloaded). (a) Low magnification. (b) High magnification of region (b). (c) High magnification of region (c). (d) High magnification of region (d).

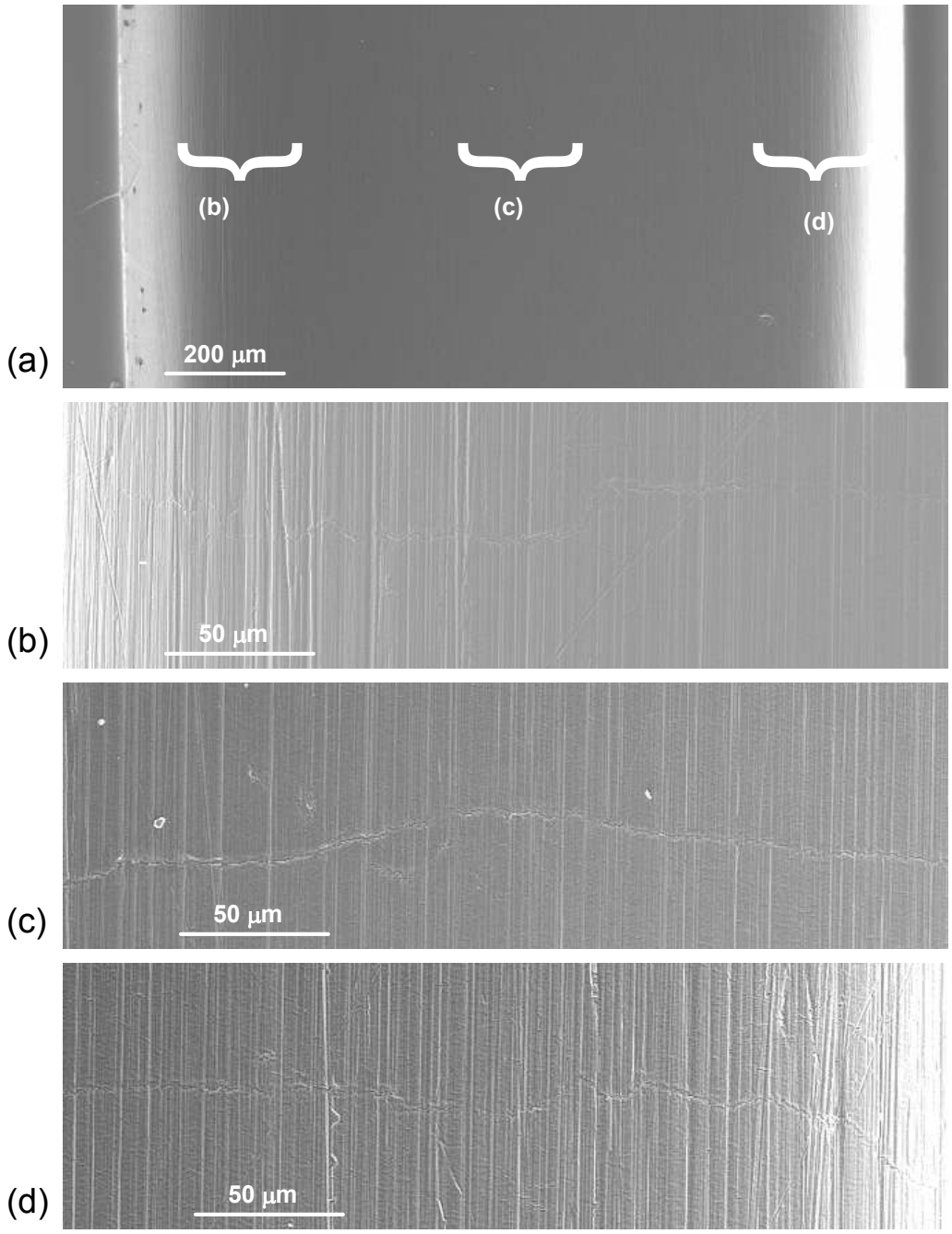

Figure 29. SEM images of specimen C2 after polishing (unloaded). (a) Low magnification. (b) High magnification of region (b). (c) High magnification of region (c). (d) High magnification of region (d).

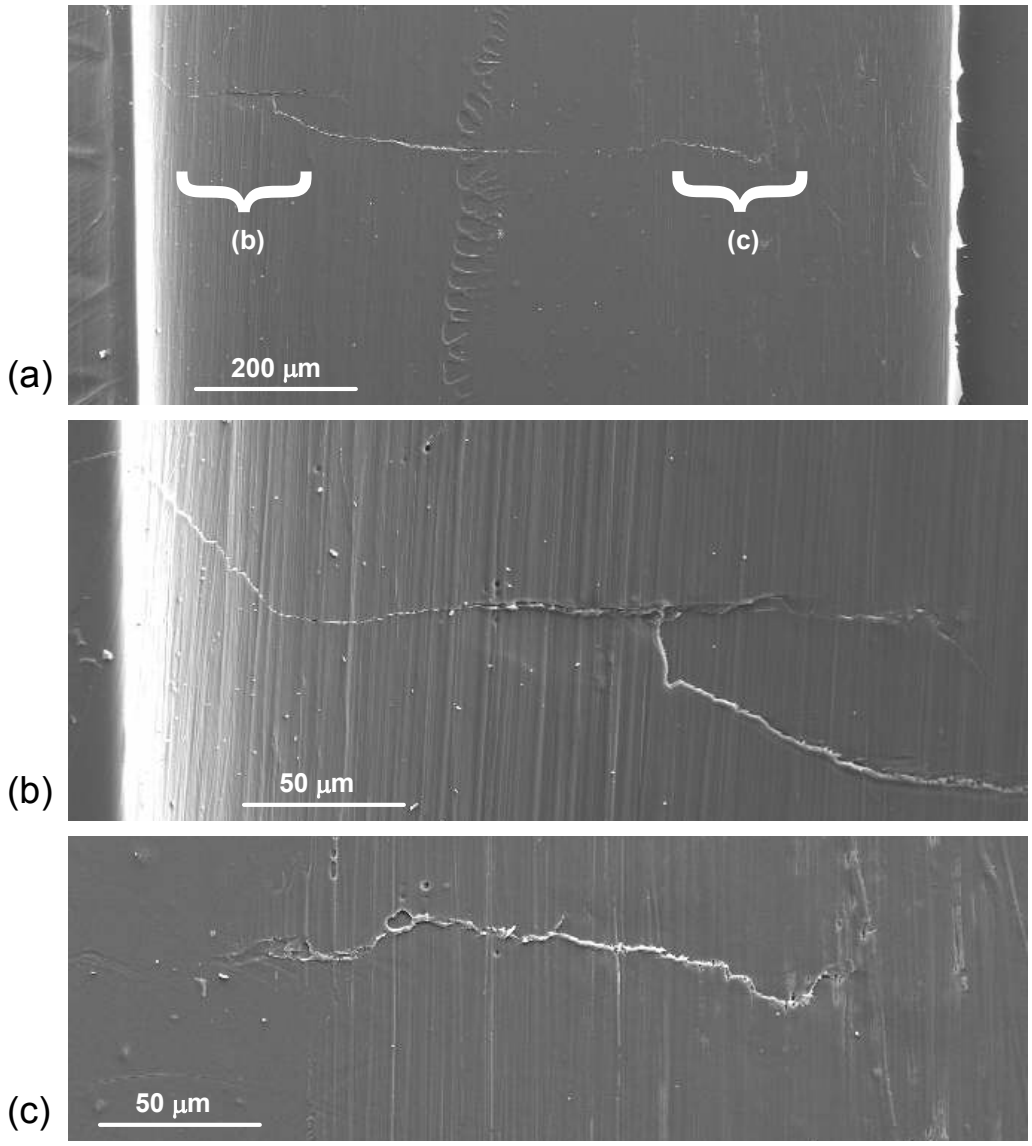

Figure 30. SEM images of specimen C9 before polishing (unloaded). (a) Low magnification. (b) High magnification image of region (b). (c) High magnification image of region (c).

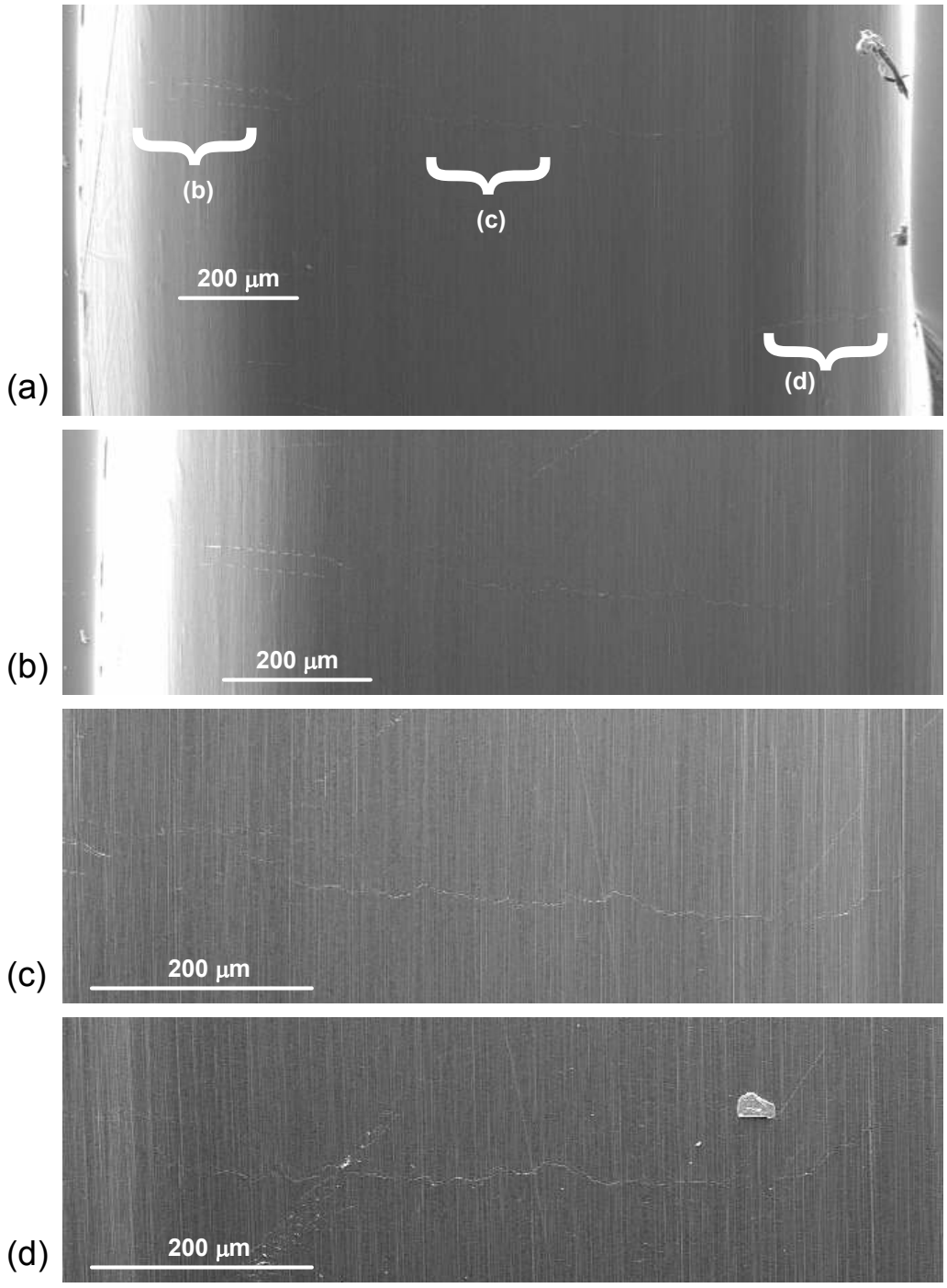

Figure 31. SEM images of specimen C9 after polishing (unloaded). (a) Low magnification. (b) High magnification image of region (b). (c) High magnification image of region (c). (d) High magnification of region (d).

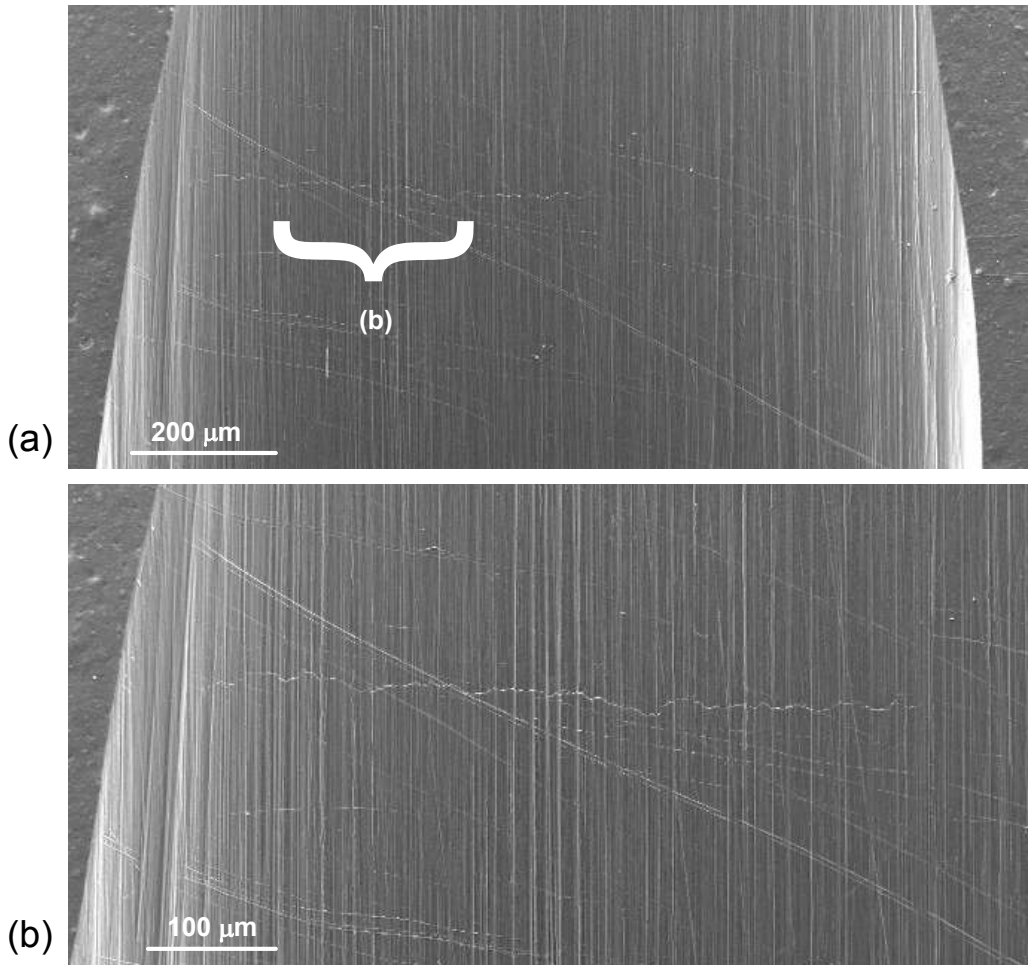

Figure 32. SEM images of specimen C12 before polishing (unloaded). (a) Low magnification. (b) High magnification image of region (b).

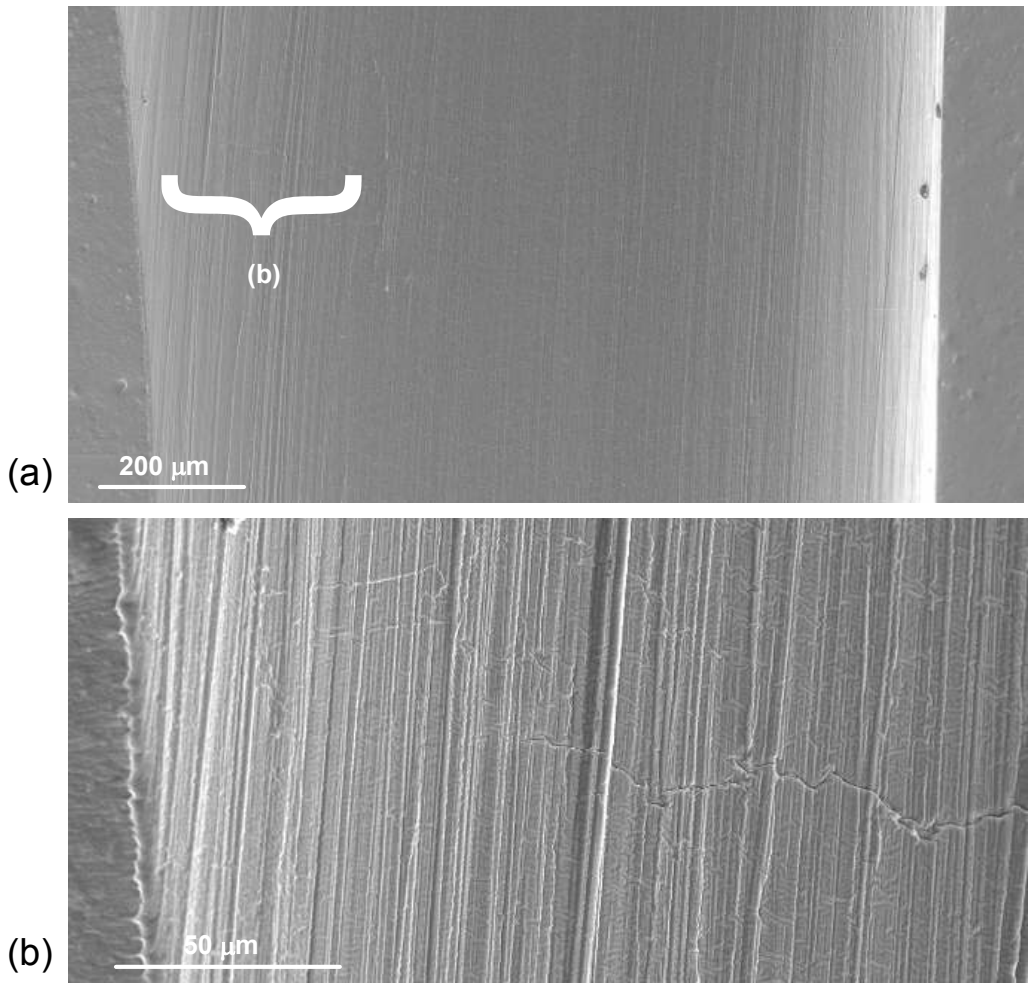

Figure 33. SEM images of specimen C13 before polishing (unloaded). (a) Low magnification. (b) High magnification image of region (b).

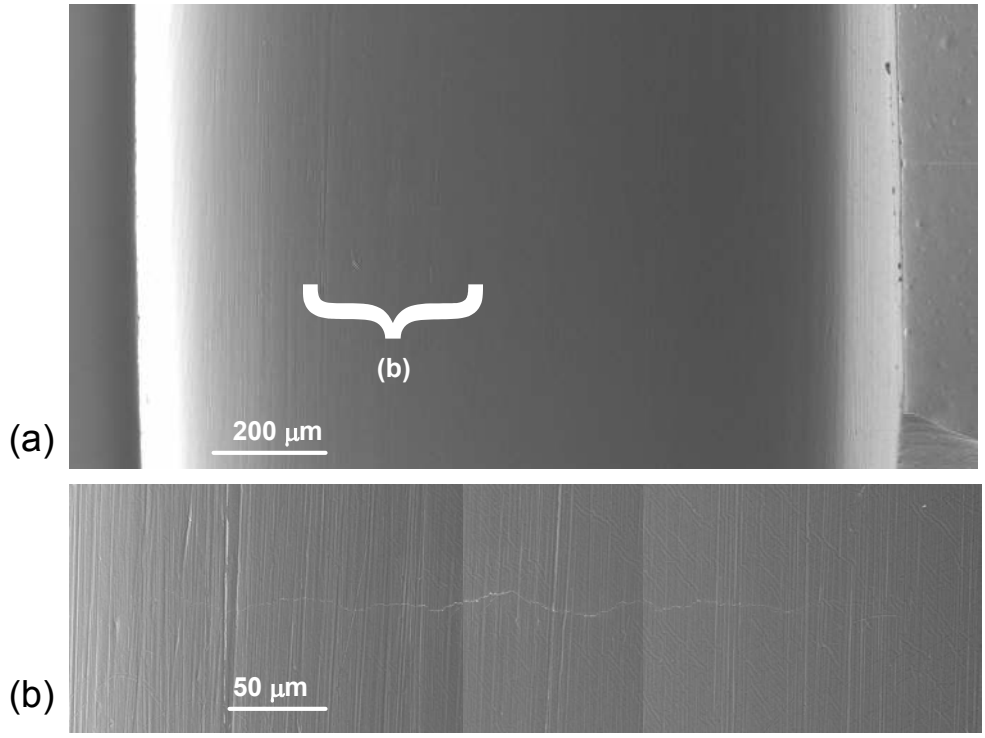

Figure 34. SEM images of specimen C12 after polishing, loaded to a notch stress of 50 ksi. (a) Low magnification. (b) High magnification image of region (b).

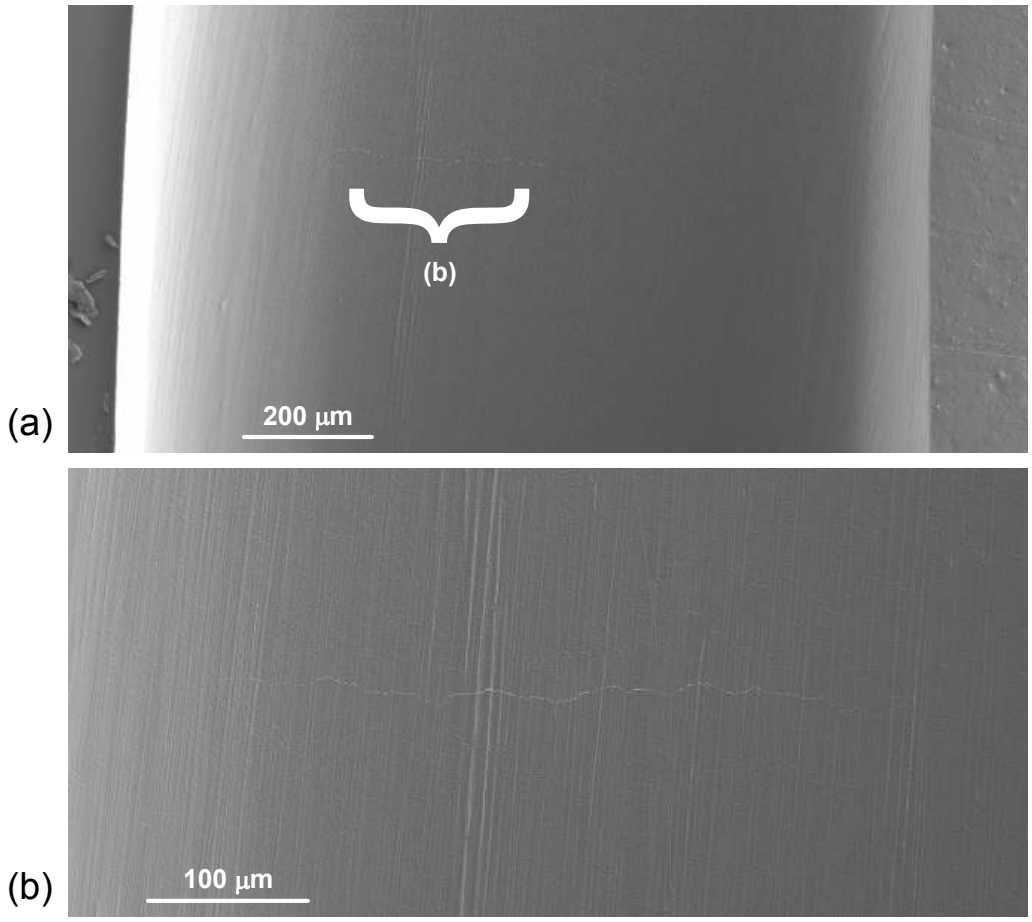

Figure 35. SEM images of specimen C13 after polishing, loaded to a notch stress of 160 ksi. (a) Low magnification. (b) High magnification image of region (b).

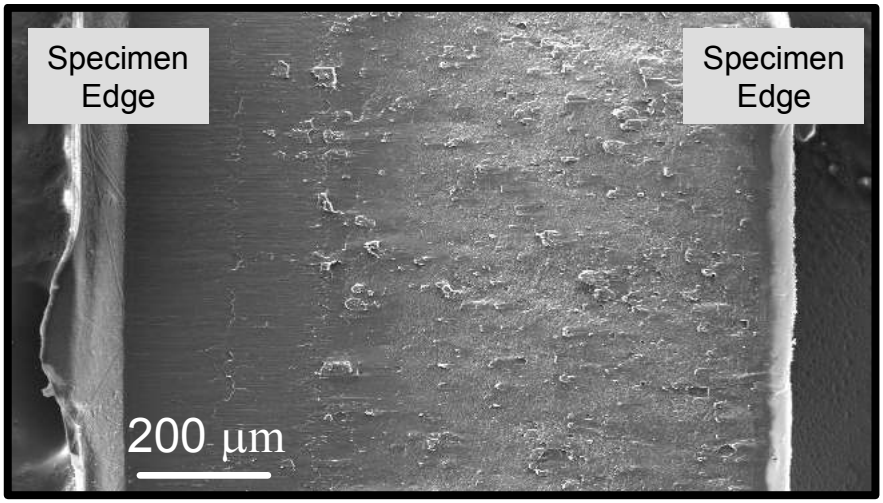

Figure 36. SEM image (acetate replica) showing the rough morphology of as-punched slot surfaces.

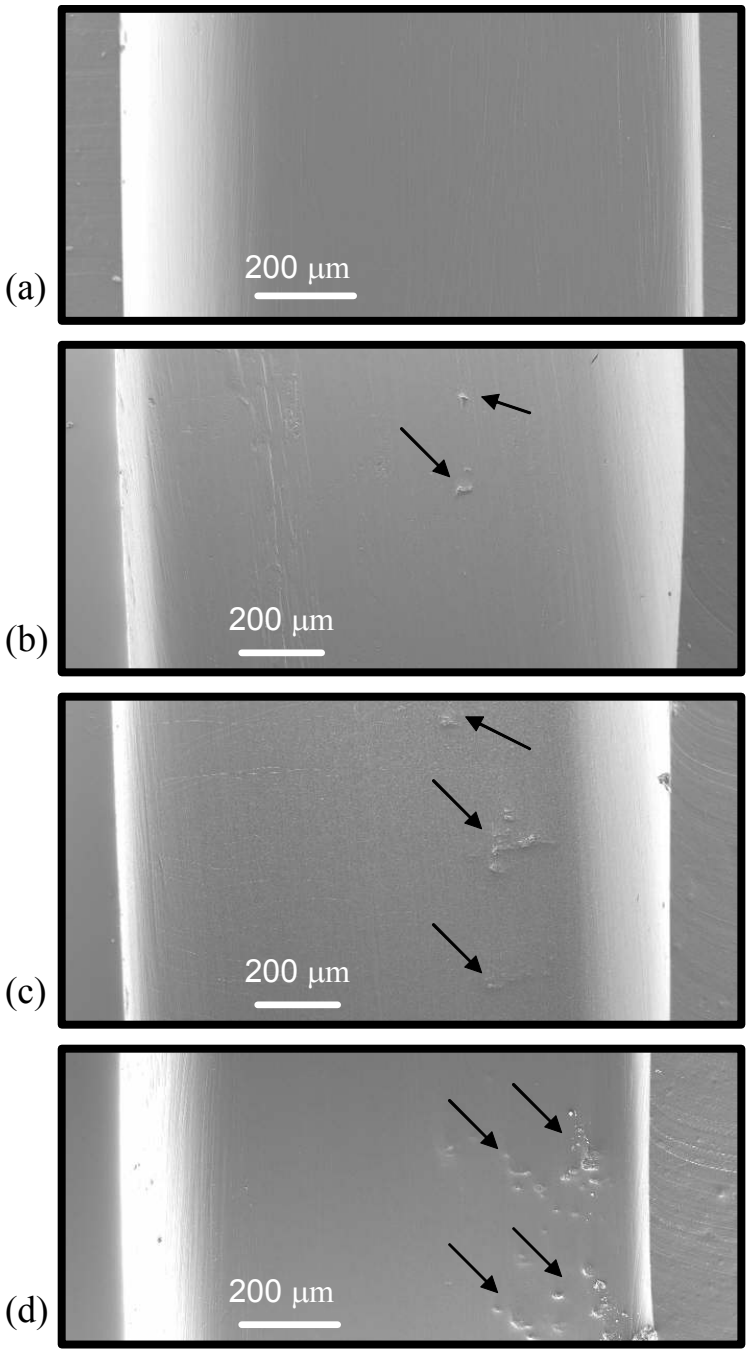

Figure 37. SEM images (acetate replicas) of four slot surfaces that were polished using the flight-hardware-approved polishing method are shown. (a) No visible damage. (b) Localized single pit damage. (c) Localized multi-pit damage. (d) Widespread pit damage.

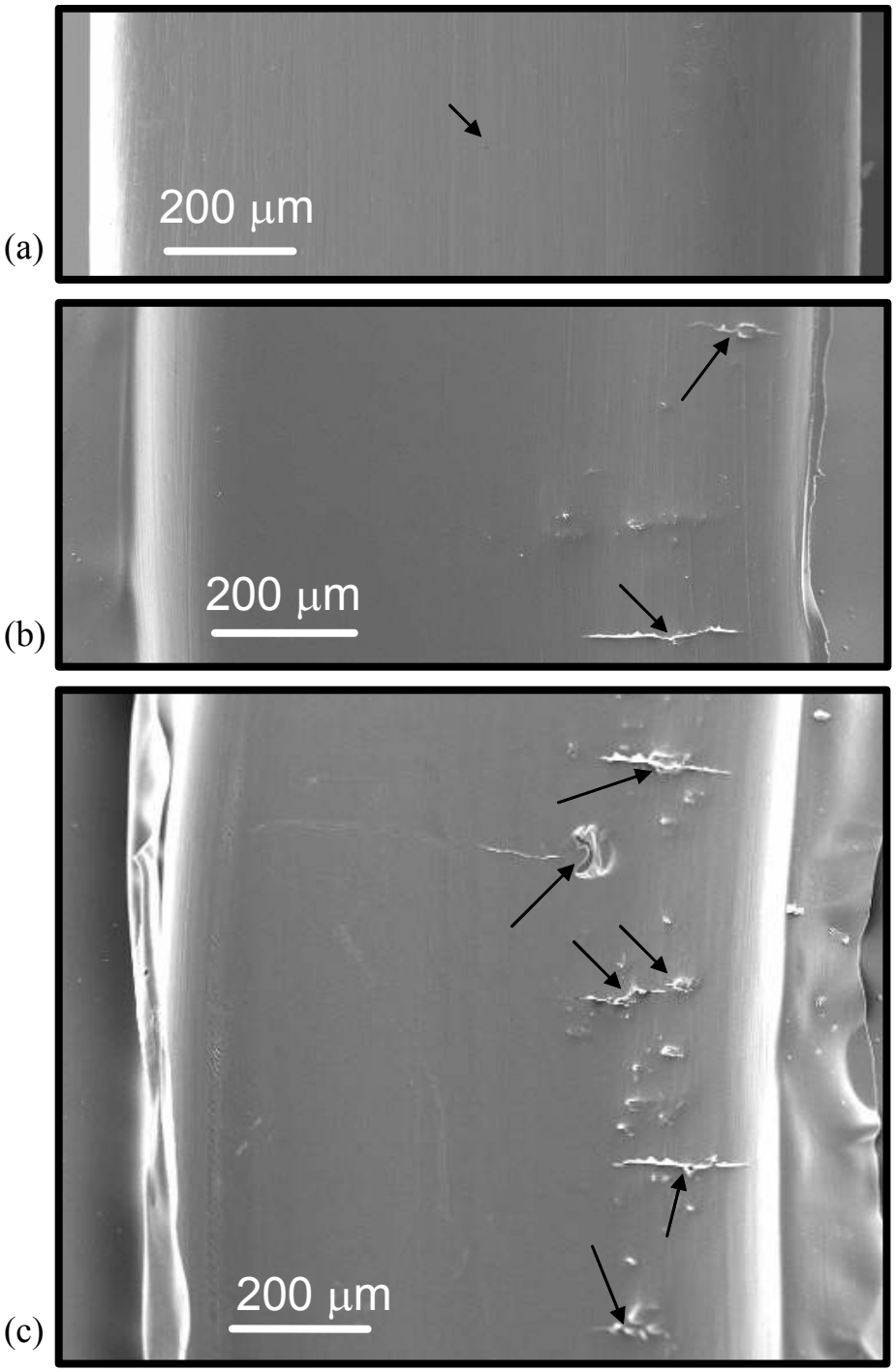

Figure 38. SEM images (acetate replicas) showing the effects of surface finish quality on fatigue-crack-initiation life. (a) For a high-quality finish (specimen P2), a single 0.005-inch-long surface crack was found after 115,000 cycles. (b) For localized single-pit damage (specimen C8), two surface cracks (0.008 and 0.005 inches long) were found at 50,000 cycles. (c) For widespread fatigue damage (specimen C6), at least seven cracks were found at 50,000 cycles; three cracks were 0.008 inches long.

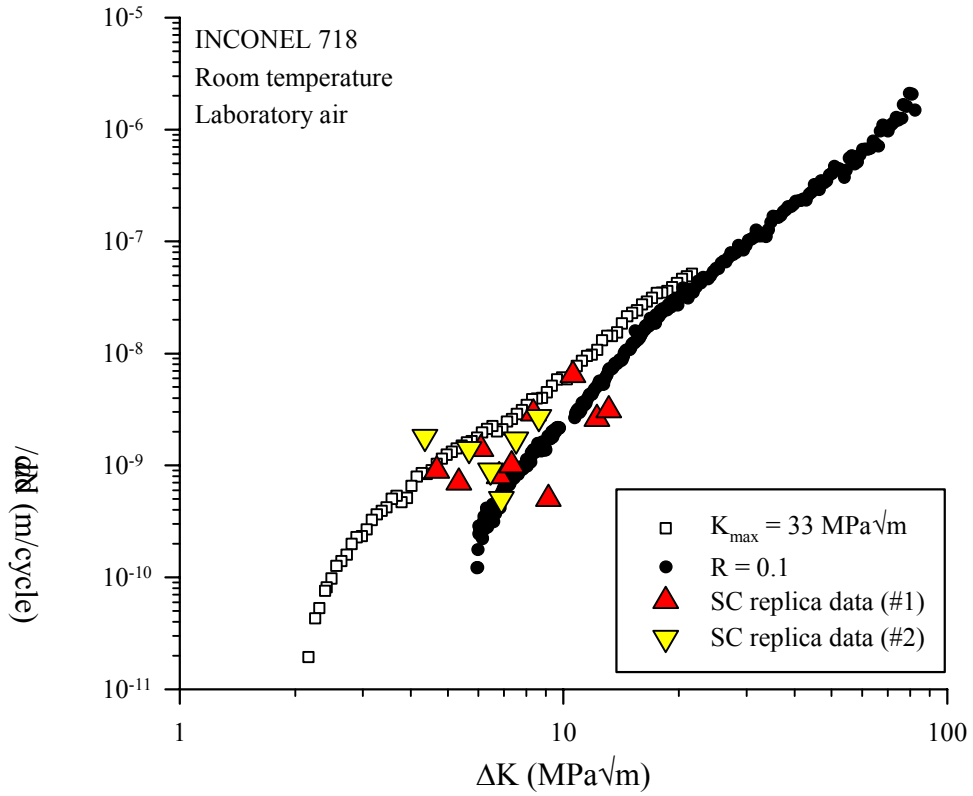

Figure 39. Small crack growth data and long crack growth data are plotted together for comparison.

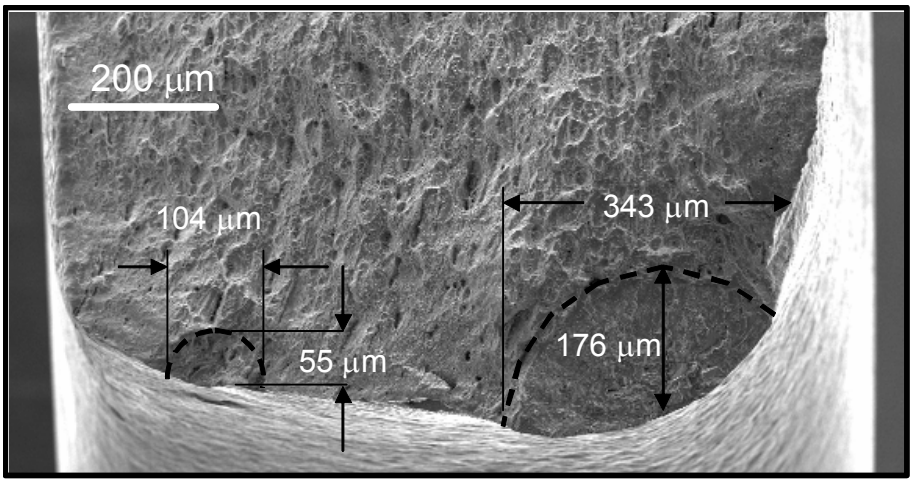

Figure 40. SEM micrograph of crack surfaces for specimen P1.

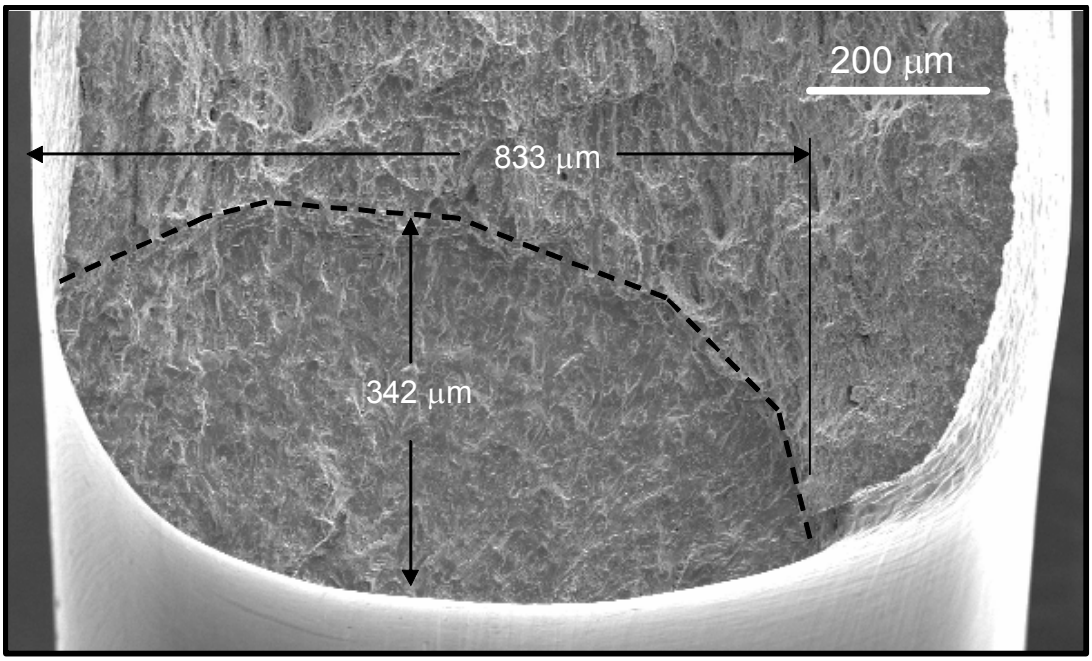

Figure 41. SEM micrograph of crack surface for specimen C9.

REPORT DOCUMENTATION PAGE

Form Approved
OMB No. 0704-0188

The public reporting burden for this collection of information is estimated to average 1 hour per response, including the time for reviewing instructions, searching existing data sources, gathering and maintaining the data needed, and completing and reviewing the collection of information. Send comments regarding this burden estimate or any other aspect of this collection of information, including suggestions for reducing this burden, to Department of Defense, Washington Headquarters Services, Directorate for Information Operations and Reports (0704-0188), 1215 Jefferson Davis Highway, Suite 1204, Arlington, VA 22202-4302. Respondents should be aware that notwithstanding any other provision of law, no person shall be subject to any penalty for failing to comply with a collection of information if it does not display a currently valid OMB control number.
PLEASE DO NOT RETURN YOUR FORM TO THE ABOVE ADDRESS.

1. REPORT DATE *(DD-MM-YYYY)*	2. REPORT TYPE	3. DATES COVERED *(From - To)*
01- 02 - 2006	Technical Memorandum	

4. TITLE AND SUBTITLE

Flow Liner Slot Edge Replication Feasibility Study

5a. CONTRACT NUMBER

5b. GRANT NUMBER

5c. PROGRAM ELEMENT NUMBER

6. AUTHOR(S)

Newman, John A.; Willard, Scott A.; Smith, Stephen W.; and Piascik, Robert S.

5d. PROJECT NUMBER

5e. TASK NUMBER

5f. WORK UNIT NUMBER

762-60-61-09

7. PERFORMING ORGANIZATION NAME(S) AND ADDRESS(ES)

NASA Langley Research Center
Hampton, VA 23681-2199

U.S. Army Research Laboratory
Vehicle Technology Directorate
NASA Langley Research Center
Hampton, VA 23681-2199

8. PERFORMING ORGANIZATION REPORT NUMBER

L-19181

9. SPONSORING/MONITORING AGENCY NAME(S) AND ADDRESS(ES)

National Aeronautics and Space Administration
Washington, DC 20546-0001 and
U.S. Army Research Laboratory
Adelphi, MD 20783-1145

10. SPONSOR/MONITOR'S ACRONYM(S)

NASA

11. SPONSOR/MONITOR'S REPORT NUMBER(S)

NASA/TM-2006-213921 ARL-TR-3638

12. DISTRIBUTION/AVAILABILITY STATEMENT

Unclassified - Unlimited
Subject Category 26
Availability: NASA CASI (301) 621-0390

13. SUPPLEMENTARY NOTES

An electronic version can be found at http://ntrs.nasa.gov

14. ABSTRACT

Surface replication has been proposed as a method for crack detection in space shuttle main engine flowliner slots. The results of a feasibility study show that examination of surface replicas with a scanning election microscope can result in the diction of cracks as small as 0.005 inch, and surface flaws as small as 0.001 inch, for the flowliner material.

15. SUBJECT TERMS

Surface replicas; Crack detection; Flowliner; Space shuttle; Hydrogen feedline

16. SECURITY CLASSIFICATION OF:			17. LIMITATION OF ABSTRACT	18. NUMBER OF PAGES	19a. NAME OF RESPONSIBLE PERSON
a. REPORT	b. ABSTRACT	c. THIS PAGE			STI Help Desk (email: help@sti.nasa.gov)
					19b. TELEPHONE NUMBER *(Include area code)*
U	U	U	UU	57	(301) 621-0390